The Journal of Neuroscience, November 1, 1996, *16*(21):6807–6829

Amino Acid Signatures in the Primate Retina

Michael Kalloniatis,[1] Robert E. Marc,[2] and Ralph F. Murry[2]

[1]*Department of Optometry and Vision Sciences, University of Melbourne, Parkville, Victoria 3052, Australia, and* [2]*John Moran Eye Center, University of Utah, Salt Lake City, Utah 84132*

Pattern recognition of amino acid signals partitions virtually all of the macaque retina into 16 separable biochemical theme classes, some further divisible by additional criteria. The photoreceptor→bipolar cell→ganglion cell pathway is composed of six separable theme classes, each possessing a characteristic glutamate signature. Neuronal aspartate and glutamine levels are always positively correlated with glutamate signals, implying that they largely represent glutamate precursor pools. Amacrine cells may be parsed into four glycine-dominated (including one glycine/GABA immunoreactive population) and four GABA-dominated populations. Horizontal cells in central retina possess a distinctive GABA signature, although their GABA content is constitutively lower than that of amacrine cells and shows both regional and sample variability. Finally, a taurine–glutamine signature defines Müller's cells. We thus have established the fundamental biochemical signatures of the primate retina along with multiple metabolic subtypes for each neurochemical class and demonstrated that virtually all neuronal space can be accounted for by cells bearing characteristic glutamate, GABA, or glycine signatures.

Key words: immunocytochemistry; neurotransmitters; retina; primate; vision; glutamate; GABA; glycine; taurine; aspartate; glutamine; pattern recognition

The fast neurotransmitters glutamate, GABA, and glycine dominate retinal information processing (Yazulla, 1986; Ehinger, 1989; Marc, 1989; Marc et al., 1990, 1995; Massey, 1990; Davanger et al., 1991; Crooks and Kolb, 1992; Kalloniatis and Fletcher, 1993; Kalloniatis and Napper, 1996). At least one of these neurotransmitter candidates can be localized in virtually every retinal neuron in chicken and goldfish retinas (Kalloniatis and Fletcher, 1993; Marc et al., 1995), and unique biochemical categories of neurons and glia have thus been defined. In this work, we have explored whether these nonmammalian patterns of biochemical grouping were generic and extensible to a key mammalian model: the primate retina. The problem of assigning amino acids to cellular compartments is daunting: the primate retina possesses more than 50 unique neuronal types, many of which are distinguishable exclusively by solitary neuron marking methods (Wässle and Boycott, 1991; Kolb et al., 1992). Our prime objective in this work was to develop a fundamental atlas of primate retinal neurochemistry.

Pattern recognition of multiple cellular signals probed by amino acid-specific IgGs is a robust method for grouping cells into statistically separable sets (Marc et al., 1995), and we now demonstrate that >99% of cellular space in the central retina of cynomologous macaques maps into unique glutamate-, GABA-, or glycine-dominated neuronal classes and taurine-rich glia. These classes broadly resemble those described for nonmammalian retinas augmented by additional "mammalian" phenotypes. Analysis of amino acid signatures reveals that nominally glutamatergic bipolar and ganglion cells each exist in several distinct neurochemical forms. Likewise both GABA- and glycine-dominated amacrine cells display diverse metabolic signatures that partition them into biochemical subsets, including class **G2**, which corresponds to type AII amacrine cells. As in nonmammalians, presumed GABAergic central horizontal cells constitute a distinctive cell cohort. Only in the far periphery do we find a small proportion of amacrine cells lacking GABA, glycine, or glutamate signals. The distribution of glutamine and aspartate signals supports a primary precursor role for these amino acids.

MATERIALS AND METHODS

Tissue preparation and immunocytochemistry. Cynomologous monkey retinas were obtained from Dr. Louis DeSantis, Alcon Laboratories (Fort Worth, TX) (monkey 571, 5+-yr-old male), and the Commonwealth Serum Laboratory (Parkville, Australia) (monkey M378, 2-yr-old male). Monkey 571 was euthanized with Nembutal; monkey M378 and others were deeply anesthetized, and after tissue harvest were euthanized by thoracotomy. Open eyecups were then fixed in cold 1% paraformaldehyde, 2.5% glutaraldehyde, 3% sucrose, 0.01% $CaCl_2$, in 0.1 M phosphate buffer, pH 7.4. Most analyses from monkey 571 were taken ~1-3 mm temporal to the fovea, just below the horizontal meridian. Various retinal samples were analyzed from monkey M328, including the fovea, midperiphery, and far periphery. All tissue was processed as described previously (Kalloniatis and Fletcher, 1993; Marc et al., 1995). This study encompasses analyses from five locations: the foveal pit, 1 mm from the pit, 1–3 mm from the pit, ≈4-6 mm inferior to the fovea, and ≈8-10 mm superior to the fovea.

The post-embedding immunocytochemical procedures used here were as described previously (Marc et al., 1990, 1995; Kalloniatis and Fletcher, 1993). IgGs from Chemicon International (Temecula, CA) and those produced by the Marc laboratory (Marc et al., 1995) targeted glutaraldehyde-conjugate haptens: L-aspartate, L-glutamate, L-glutamine, glycine, GABA, L-serine, and taurine. Primary IgG signals were detected with goat-anti-rabbit IgGs coated with 1 nm gold particles, as detailed previously, and visualized with silver intensification.

Nomenclature. We use the conventional single-letter code for the natural amino acids augmented by a Greek notation for the nonprotein amino acids (Marc et al., 1995): glutamate = E, GABA = γ, glycine = G, taurine = τ, aspartate = D, glutamine = Q, and serine = S. A serial

Received June 24, 1996; revised Aug. 1, 1996; accepted Aug. 14, 1996.

This work was supported by National Health and Medical Research Council Grant 940087 (M.K.), American Red Cross Grant S0969325 (M.K.), National Institutes of Health Grants EY02576 (R.E.M.) and NRSA EY06651 (R.F.M.), and a Research to Prevent Blindness Jules and Doris Stein Professorship (R.E.M.). Part of this work was conducted while Dr. Michael Kalloniatis was on Special Studies Program leave from the University of Melbourne. We thank Mr. Guido Tomisich and Ms. M. V. Shaw for technical assistance.

Correspondence should be addressed to Dr. Robert E. Marc, John Moran Eye Center, University of Utah Health Sciences Center, 50 North Medical Drive, Salt Lake City, UT 84132.

section analysis of glutamate, GABA, glycine, taurine, aspartate, and glutamine signals, respectively, is thus defined as the EγGτDQ six-dimensional set. Binary signal patterns are referred to as GABA, glycine, or glutamate, positive and negative: γ^+, γ^-, G^+, G^-, E^+, and E^-. Characterization of outcomes in terms of theme classes (see below) uses a bold, upper-case letter notation for the dominant presumed functional molecules of a theme class and ordinal notation for subsets: glutamate = **E1**, **E2**. . . **En**; GABA = **Γ1**, **Γ2**. . . **Γn**; glycine = **G1,G2**. . . **Gn** and **GΓ1**; and taurine = **T1**.

Image calibration, signal interpretation, and image registration. Images of immunoreactivity were captured under constant flux 550 nm (10 nm bandpass) light using fixed camera gain and γ, yielding a log-linear pixel value (PV) scale over the usable irradiance, and stored as 512 pixel × 480 line image frames. For practical purposes, PV scales linearly with log concentration in our system over a 2-log unit range. Images from single sections were montaged, and each montage from a series of sections was aligned; both operations were achieved by conventional image registration methods (EASI/PACE software from PCI Remote Sensing, Richmond Hill, Ontario, Canada), using common anatomical landmarks as control points. Most images were registered with >250 nm root mean square error. Low-pass filtering was performed to suppress intracellular variations arising from intracellular inclusions. All images were inverted using a logical NOT operation so that increasing immunoreactivity scaled with increasing PV. Details of these methods are available in Marc et al. (1995).

Image visualization, pattern recognition, and statistical analysis. Image analysis data can be explored in two ways (Richards, 1993): (1) visual inspection of *rgb* mapped images and (2) quantitative analyses in which computational methods such as pattern recognition are used to extract statistical attributes. Common points on registered images represent formal lists of amino acid signals linked to a specific structure in anatomical space; the key objective is to explore these lists and search for correlated patterns of amino acid content. A basic exploration of correlations among amino acid contents is achieved by viewing the images as doublets or triplets after assigning one amino acid image to one color channel of a video monitor. This is amino acid→red, green, blue triplet (*rgb*) mapping; however, *rgb* mapping is not a statistical method and must be augmented with more quantitative tools. In this paper we use pattern recognition methods to explore N-dimensional amino acid data and extract statistically separable and/or significant cell classes. The complementary roles and limits of visual inspection and pattern recognition in exploring amino acid signatures have been elaborated previously (Marc et al., 1995). In this study, amino acid→*rgb* mappings of registered serial sections were inspected to delimit profitable regions for pattern recognition analysis. K-means extraction of theme classes based on amino acid signatures was performed on all five retinal eccentricities outlined above, and theme maps were constructed for each (not all data are shown). Theme classes are formal groupings based solely on common sets of signal values and intervalue correlations, not on anatomical features. The actual sets of amino acid signals for each class were viewed as bivariate scatter plots with bounding 2 SD bivariate ellipses and univariate probability histograms. The latter were FFT-filtered, yielding a concentration difference resolution of 0.125 log units over a 2-log unit concentration range.

The statistical basis of pattern recognition is discussed in Swain and Davis (1978). A clear distinction between *significant* classes and *separable* classes is important. *Significant* classes are those whose univariate or multivariate distribution of signals clearly cannot be derived from the same population, although they may overlap greatly. Rods and cones are an example of this situation. They are morphologically separable and we can show, by conventional parametric tests (Student's *t*) of one or more univariate amino acid histograms, that they represent sets drawn from different distributions in sample space with $p \ll 0.01$. These classes, however, are not *separable*. Statistical *separability* requires that some combination of N-means and covariances leads to <1% error (a selected criterion) in classifying a sample of N signals. Thus we can examine the results of K-means clustering for their *significances* and their *separabilities*. Separable classes are significant classes; the converse is not always true. The separability of theme classes is reported as transformed divergence (D^T), a statistic for estimating the degree of pairwise theme class segregation (Swain and Davis, 1978). The standard cutoff for significance is $D^T \geq 1.9$, corresponding to a probability of error $p_e < 0.01$ for populations with equal a priori probability density functions. Most theme classes were fully separable with $D^T \geq 1.9$, but three pairs of significant classes had $D^T < 1.9$: **E1/E1′, E2/E2′**, and **Γ2/Γ2′**. The origins of these subsets will be examined in Results.

Basic cell identification. The cellular identities of biochemical classes were assessed by correlating theme classes with registered toluidine blue-stained 250 nm sections. Nominal bipolar cells were defined by their distinctive ovoid profiles and scant cytoplasm and their homogenous and strongly basophilic nuclei. In optimal circumstances, bipolar cell axons or primary dendrites could be traced to the inner plexiform or outer plexiform layers, respectively. Horizontal cell somas positioned at the proximal face of the outer plexiform layer were distinguished by large, round, pale nuclei and abundant cytoplasm. Finally, nominal amacrine cells were positioned at, or one cell diameter from, the distal face of the inner plexiform layer and were stained with distinctive weak basophilia, often displaying heterogeneous chromatin staining and indented nuclei. The extents to which these traditional groups are corrupted by inappropriate inclusions are unknown, but theme classes extracted by pattern recognition were homogenous in terms of their toluidine blue identifications. Characterization of interplexiform cells was not possible. Identification of displaced amacrine cells is based on our assumption that sparse populations of cells positioned in the first row of the ganglion cell layer and possessing the same γ^+ signature as a large number of conventional amacrine cells are likely to be bona fide amacrine cells. None of these groupings, however, has been confirmed by electron microscopic or other unequivocal means and must be acknowledged as presumptive. In summary, theme classes arise exclusively from biochemical signals and do not depend on morphological identities. After theme classes are extracted, they may be correlated directly with light microscopic data for basic cell identifications.

RESULTS

General amino acid localization in the primate retina

Retinal glutamate, GABA, and glycine immunoreactivities generally follow those described previously in primate retinas (Hendrickson et al., 1988; Grünert and Wässle, 1990; Davanger et al., 1991; Grünert and Martin, 1991; Crooks and Kolb, 1992; Martin and Grünert, 1992; Robin and Kalloniatis, 1992; Koontz et al., 1993). In previous work, glutamate immunoreactivity has been one of the most variable amino acid signals (e.g., Davanger et al., 1991; Crooks and Kolb, 1992; Martin and Grünert, 1992). We found small variations in glutamate signal strength in samples from different animals reported here, but the *pattern* of distributions was extremely stable. In our experience, tissue collected from monkeys after use in chronic electrophysiological experiments (none reported here) showed substantial and unacceptable variability in glutamate signals (Kalloniatis et al., 1994b). Although not the focus of this work, glutamate signals in particular seem likely to be indices of recent physiological or pathophysiological history in neural tissue samples. Thus the homogeneity of glutamate signals that we observe within classes gives us confidence that most of our data reflect normal steady-state conditions.

Most retinal neurons displayed some glutamate content (Fig. 1*A*), with ganglion cells and their axons containing the highest levels. Foveal cones display glutamate levels comparable to those of ganglion cells, but at most other eccentricities rods show higher glutamate levels than cones. Bipolar and amacrine cells show very similar glutamate levels, whereas horizontal cells and Müller's cells are either glutamate-immunonegative or possess a very low glutamate signal that borders on the threshold of detection (<100 μM; Marc et al., 1990).

Many amacrine cells exhibit strong GABA signals (≥10 mM), whereas central horizontal cells, a small subset of bipolar cells, and other somas in both the amacrine and ganglion cell layers display lower values (Fig. 1*B*; also see Martin and Grünert, 1992). The stratification of GABA signals in the inner plexiform layer is almost confluent and certainly overlaps the distributions of $GABA_A$ receptors in the monkey inner plexiform layer (Grünert et al., 1993). GABA signals in Müller's cells were at background

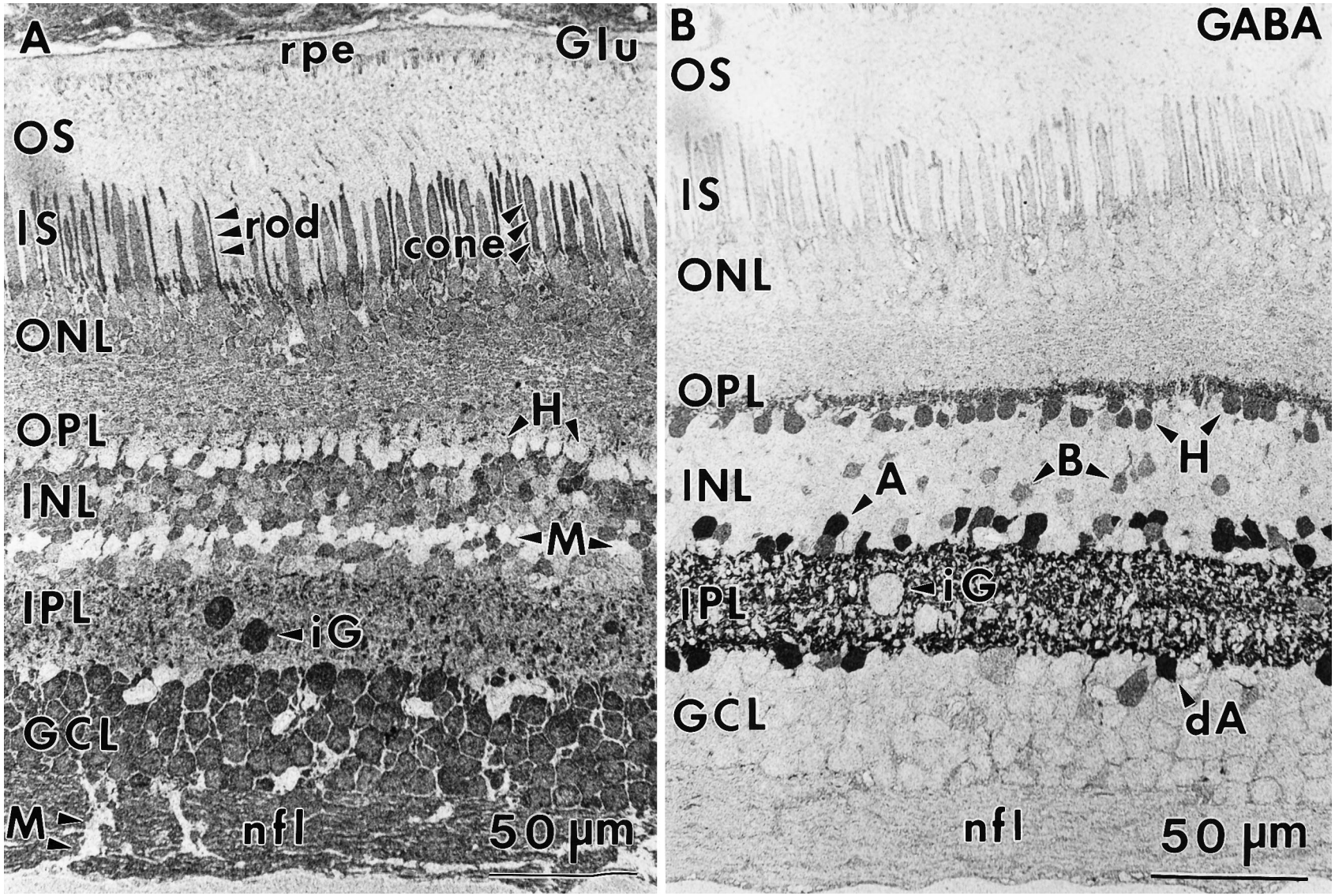

Figure 1. Glutamate (*Glu*) and GABA immunoreactivity (sample 571) 1–3 mm from the fovea. *A*, Glutamate immunoreactivity is found throughout the retina, with low levels in Müller's cells, occasional conventional and displaced amacrine cells, horizontal cells, and the outer segments of photoreceptors. Note the two interstitial ganglion cells. The highest level of immunoreactivity is displayed by ganglion cells and their axons. Note the differential labeling of cones and rods. *B*, Distinctive GABA signals are present in conventional and displaced amacrine cells, all horizontal cells, and a bipolar cell subset. Note the GABA-immunonegative interstitial ganglion cells. *OS*, Outer segments; *IS*, inner segments; *ONL*, outer nuclear layer; *OPL*, outer plexiform layer; *INL*, inner nuclear layer; *IPL*, inner plexiform layer; *GCL*, ganglion cell layer; *A*, amacrine cells; *B*, bipolar cells; *H*, horizontal cells; *dA*, displaced amacrine cells; *M*, Müller's cells; *nfl*, nerve fiber layer; *iG*, interstitial ganglion cells; *rpe*, retinal pigmented epithelium.

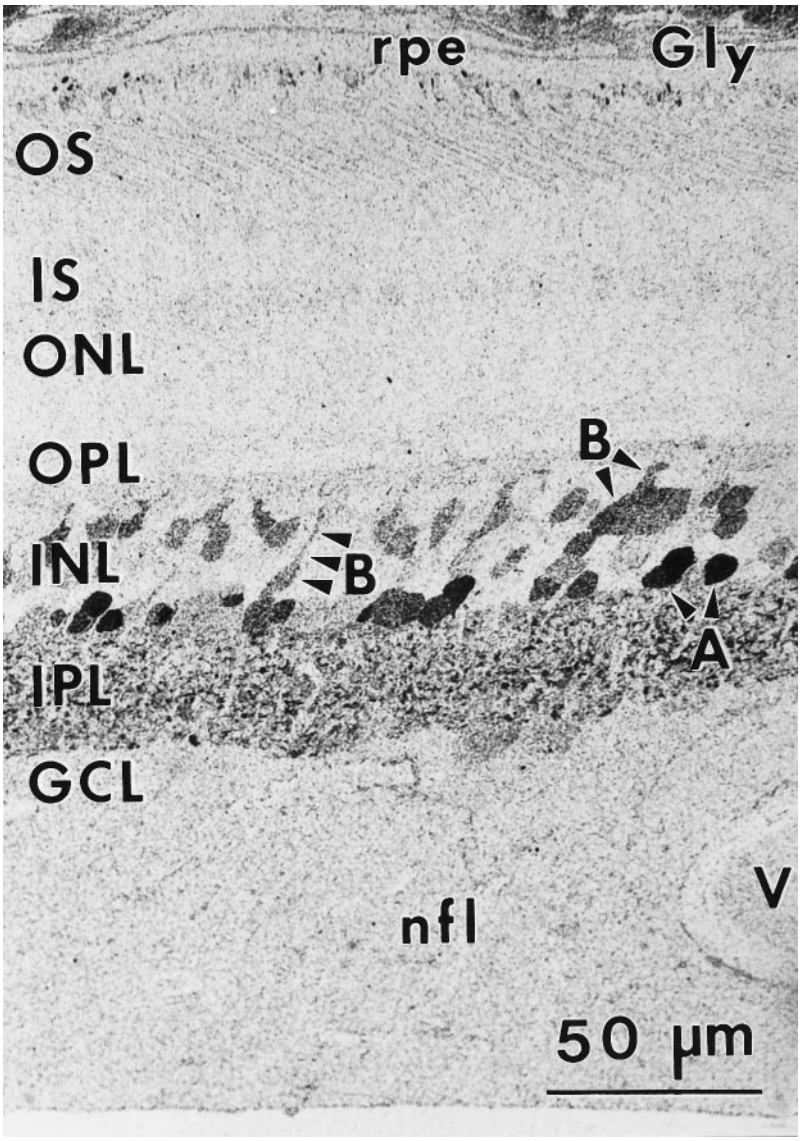

Figure 2. Glycine (*Gly*) immunoreactivity (sample 571) 1–3 mm from the fovea. Conventional amacrine cells are the predominant G^+ class. Many bipolar cells also exhibit glycine immunoreactivity, mostly in the distal inner nuclear layer (*INL*), although some cells have their somas in the Müller's cell layer. *V*, Blood vessel. Other abbreviations defined in legend to Figure 1.

levels but can be elevated quickly in acute anoxia. Horizontal cells in the central retina were not always GABA-immunoreactive in our samples, and horizontal cells and bipolar cells never label for GABA in midperiphery and beyond (see below). So far, incubating the retina briefly *in vitro* does not seem to restore GABA immunoreactivity, although both HI and HII monkey horizontal cells are immunoreactive for GAD_{65} (Vardi et al., 1994). The variability of GABA labeling in these cells is likely to reflect an extreme volatility of the GABA signal within this neural population, similar to that described for goldfish horizontal cells (Murry and Marc, 1995).

The strongest glycine signals are localized in a subset of amacrine cells with generally weaker signals in a large subset of bipolar cells (Fig. 2). We also find weak labeling in perivascular astrocytes (not shown), a finding consistent with earlier reports that these cells have an uptake system for [^{3}H]-glycine in the human retina (Marc and Liu, 1985). Displaced glycinergic amacrine cells and weakly glycine-immunoreactive ganglion cells were rare, similar to those in previous reports (Hendrickson et al., 1988).

Taurine signals are particularly intense in photoreceptors (Fig. 3*A*), often extending from the outer plexiform layer to the tips of the outer segments (Fig. 3*B*). Foveal bipolar, Müller's, and occasional amacrine cells also showed taurine immunoreactivity. Taurine-rich Müller's cell processes extend throughout the nerve fiber layer, with their end-feet forming the inner limiting membrane (Fig. 3*A*). In the peripheral retina, most of the nerve fiber layer is composed of Müller's cell end-feet (Fig. 3*B*). An increasing distal→proximal intracellular taurine signal gradient in Müller's cells at all eccentricities is likely a true taurine gradient rather than a difference in the total number of immobile matrix sites for fixation (Marc et al., 1995), because glutamine signals in the very same cells show no such gradient (Fig. 4). Horizontal cells had low taurine signals or were τ^-, especially in the periphery.

The apparent distributions of the glutamate precursors aspartate and glutamine are rather different on visual examination, but this is somewhat misleading, because Müller's cells have moderate glutamine levels and low aspartate levels. If one ignores the Müller's cell pattern, aspartate and glutamine distributions seem rather similar. Glutamine levels are quite high in ganglion cell somas, whereas their axons generally contain lower levels (Fig. 4), and this differs from glutamate, which seems uniformly partitioned in ganglion cell somas and axons. Most retinal neurons

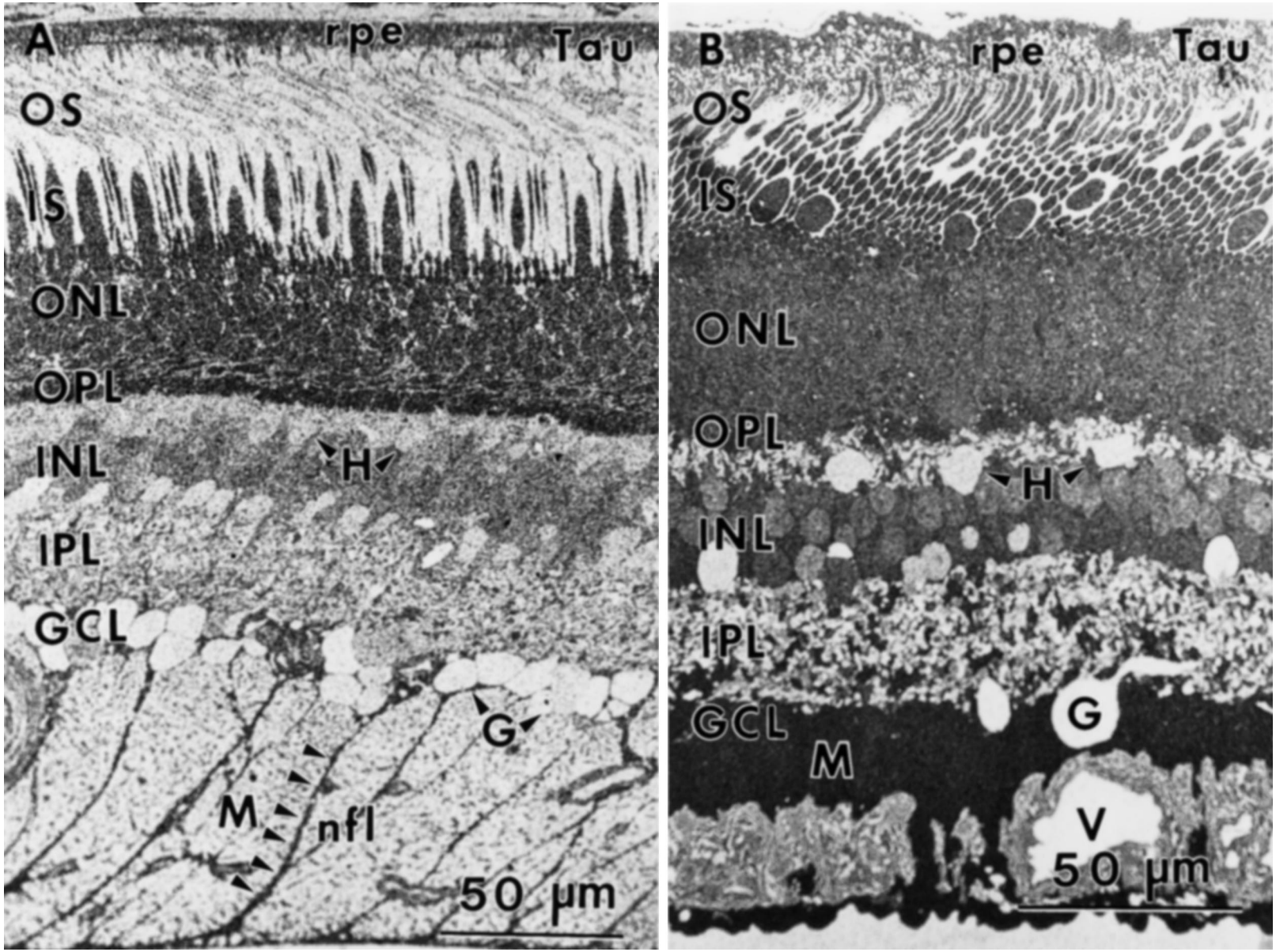

Figure 3. Taurine (*Tau*) immunoreactivity (sample 571) 1–3 mm from the fovea (*A*) and (sample M328) 8–10 mm from the fovea (*B*). *A*, Photoreceptors display the highest level of immunoreactivity, followed by bipolar cells. Müller's cell somas are indistinguishable from bipolar cells in the middle of the inner nuclear layer (*INL*); however, Müller's cell end-feet traversing the nerve fiber layer are easily identified. Note that horizontal cells (*H*) display low taurine immunoreactivity, whereas ganglion cells (*G*) are immunonegative. *B*, In the far periphery, Müller's cells dominate taurine labeling patterns in the inner nuclear and ganglion cell layers. Ganglion cells and some amacrine cells are immunonegative. *G*, Ganglion cells. Other abbreviations defined in legend to Figure 1.

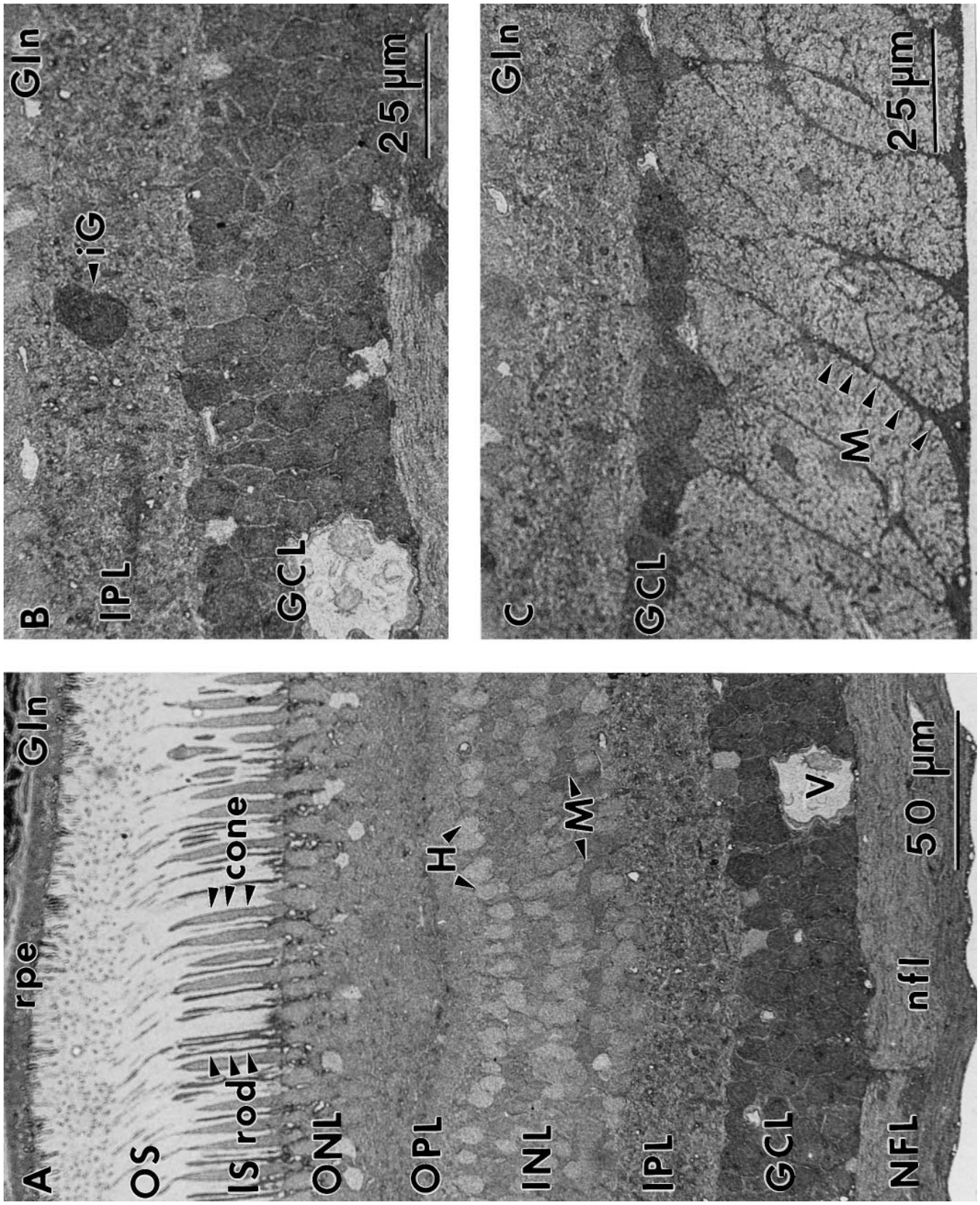
A
rpe
Gln
OS
IS rod
cone
ONL
OPL
H
INL
M
IPL
GCL
V
NFL
nfl
50 µm
B
Gln
iG
IPL
GCL
25 µm
C
Gln
GCL
M
25 µm

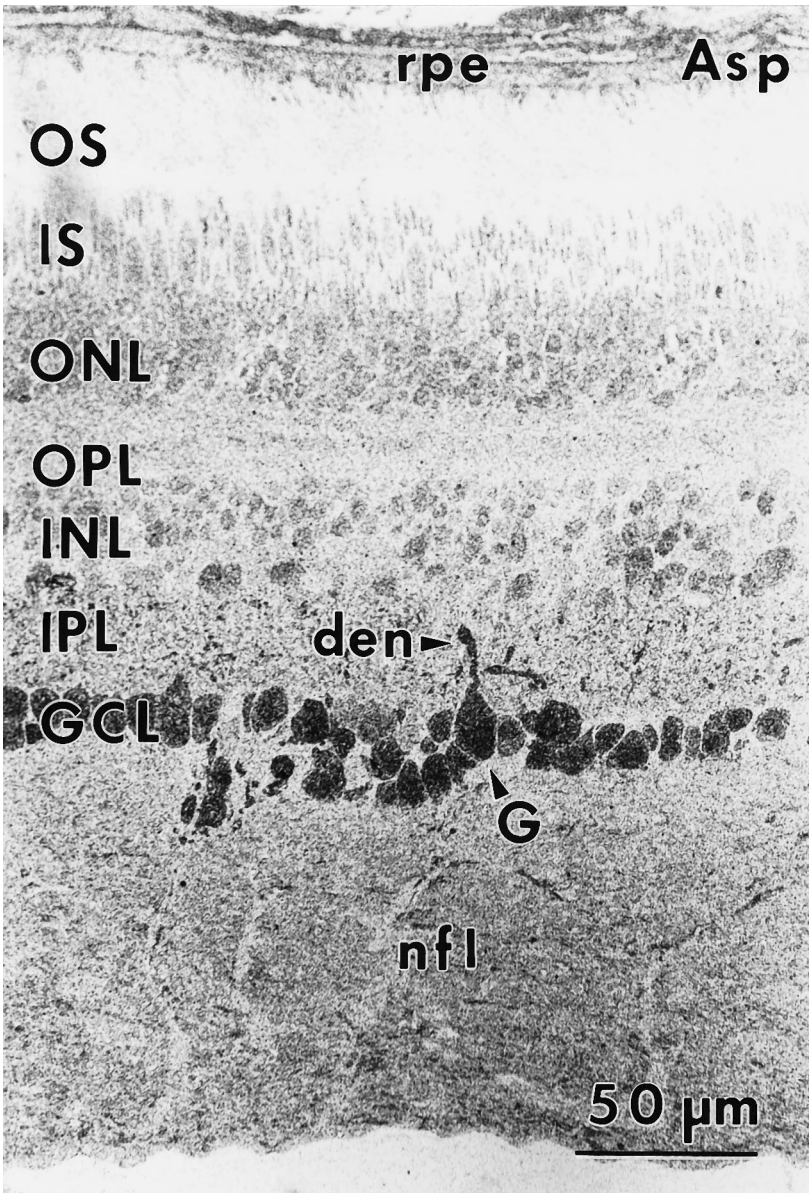

Figure 5. Aspartate (*Asp*) immunoreactivity (sample 571) 1–3 mm from the fovea. Ganglion (*G*) cell somas and dendrites (*den*) display strong aspartate labeling. A diffuse labeling pattern is present throughout the retina. Abbreviations defined in legend to Figure 1.

show some degree of glutamine content: Müller's cells have moderate levels, followed by amacrine cells and bipolar cells. Cone photoreceptors contain less glutamine than rods do, similar to their glutamate patterns, which is a partial basis for defining rods and cones as *significant* but not *separable* biochemical theme classes. The labeling pattern for glutamine in neurons generally follows that expected of a glutamate precursor, similar to the results found in other vertebrate retinas and the CNS (Shank and Campbell, 1984a,b; Ottersen et al., 1992; Kalloniatis et al., 1994a; Marc et al., 1995). As in goldfish and chicken retinas, glutamine is a good preferential label for monkey ganglion cells, with displaced amacrine cells in the ganglion cell layer showing low glutamate and glutamine signals. Aspartate signals are low in most cells, including Müller's cells, consistent with relatively lower aspartate levels in whole mammalian retina (Voaden, 1978), whereas ganglion cells have high contents. Unlike glutamate labeling, ganglion cell axons show significantly lower aspartate content than somas do (Fig. 5).

One possible pathway for CNS and retinal glycine synthesis is via serine hydroxymethyl transferase (SHMT). SHMT activity in the mammalian retina correlates roughly with glycine content (Dasgupta and Narayanaswami, 1982), and we expected to find elevated serine labeling in putative glycinergic amacrine cells, similar to the elevated glutamine and aspartate in ganglion cells. As in the goldfish retina (Marc et al., 1995), we find diffuse serine labeling in the primate retina (Fig. 6). The cytosol of ganglion

←

Figure 4. Glutamine (*Gln*) immunoreactivity (sample 571) 1–3 mm from the fovea. *A*, Ganglion cell somas display the highest level of glutamine immunoreactivity, with virtually every retinal neuron showing some degree of labeling. Note the difference in labeling between rod and cone photoreceptors and the distinctive labeling of Müller's cell somas in the inner nuclear layer (*INL*). *B*, Higher-powered photomicrograph showing the labeling pattern in the inner plexiform layer (*IPL*) and ganglion cell layer (*GCL*) and an interstitial ganglion cell. *C*, Müller's cell end-feet traversing the nerve fiber layer show morphological characteristics similar to the taurine-labeled processes noted earlier. Abbreviations defined in legend to Figure 1.

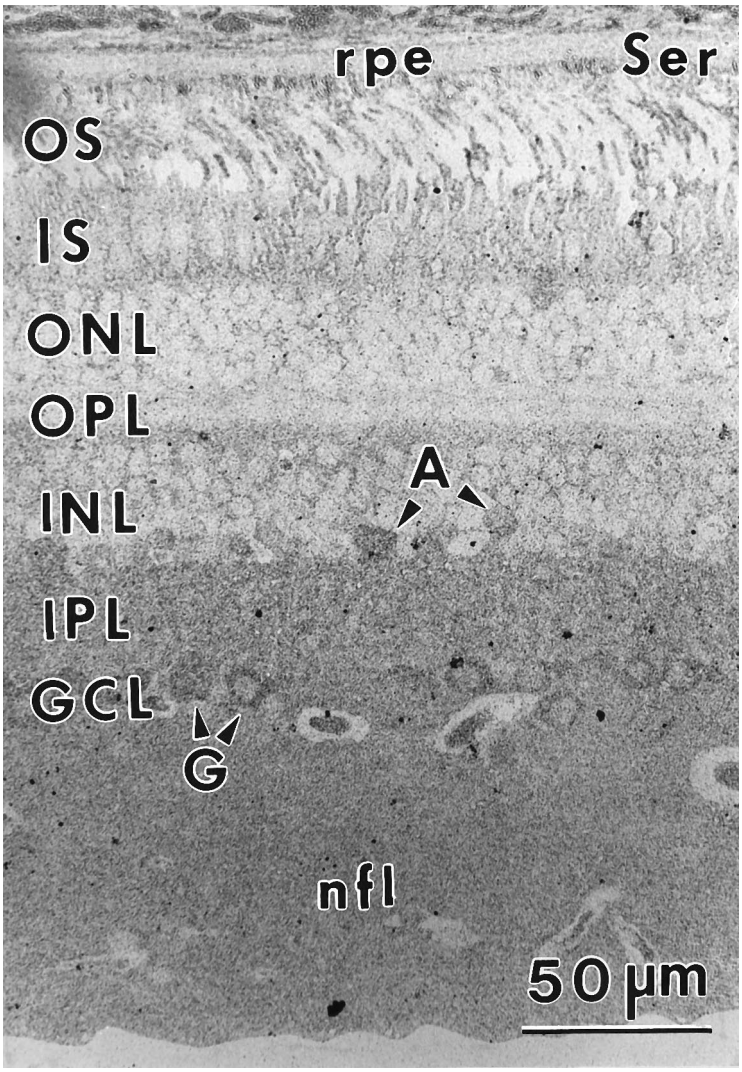

Figure 6. Serine (*Ser*) immunoreactivity (sample 571) 1–3 mm from the fovea. Diffuse labeling is found throughout the retina, with ganglion cell cytoplasm (*G*), vessel contents, the nerve fiber layer, and the occasional amacrine cell (*A*) displaying moderately higher levels of immunoreactivity. Abbreviations defined in legend to Figure 1.

cells and occasional amacrine cells show elevated labeling at levels that are comparable to that found in the nerve fiber layer, but most amacrine cells did not show selective serine labeling. The precursor role of serine for glycine production in the vertebrate retina is not supported by either this work or previous results in goldfish (Marc et al., 1995).

Although not the focus of this report, we also documented that the amino acid labeling pattern of the retinal pigmented epithelium (RPE) (Fig. 1–6) was similar to but separable from Müller's cells. RPE cells have high taurine and glutamine content and low serine, aspartate, and glutamate levels and are immunonegative for glycine and GABA. Goldfish, cat, and rabbit RPE cells (Marc et al., 1995; R. E. Marc, unpublished observation) demonstrate higher glutamate levels than those of primate RPE reported here. The high levels of immunoreactivity for these amino acids in the RPE may represent amino acid transport from the subretinal space or choroid (Miller and Steinberg, 1976; Pautler and Tengerdy, 1986; Salceda and Saldaña, 1993).

Amino acid colocalization patterns

Simple colocalization patterns allow visual identification of possible neuronal subsets and even find novel cell classes. Glutamate is the immediate precursor of GABA, and certain nonmammalian GABAergic amacrine cells display variable levels of glutamate content (Ehinger, 1989; Kalloniatis and Fletcher, 1993). Similarly, both conventional and displaced primate GABAergic amacrine cells display varied levels of glutamate (Fig. 7). It is evident that γ^+ amacrine cell subsets might exist, partly on the basis of glutamate signals (compare glutamate signals in cells *iA1* and *iA2* in Fig. 7). This is not a proof of subsets, however, and pattern recognition analysis is required to resolve such speculations. Conversely, the homogeneity of low glutamate signals in γ^+ horizontal cells establishes that certain populations display extremely low variances in their metabolite signals, as noted previously by Marc et al. (1990, 1995). This presages the characterization of statistically separable classes by pattern recognition.

Amino acid→rgb mapping

Defining cell classes by inspection is extremely subjective and increasingly challenging as more signals are compared; we thus turn to imaging methods. Serial sections probed as DEGQ$\tau\gamma$ signal sets were registered and viewed as *rgb* triplets before theme classes were extracted. Figure 8 illustrates 2 of 20 unique *rgb* triplets obtained from sample 571 at 1–3 mm from the fovea.

*Figure 8*A, *EG*γ→rgb *mapping*

This image demonstrates simultaneous localizations of glutamate, glycine, and GABA signals. E^+ photoreceptors, bipolar cells, and

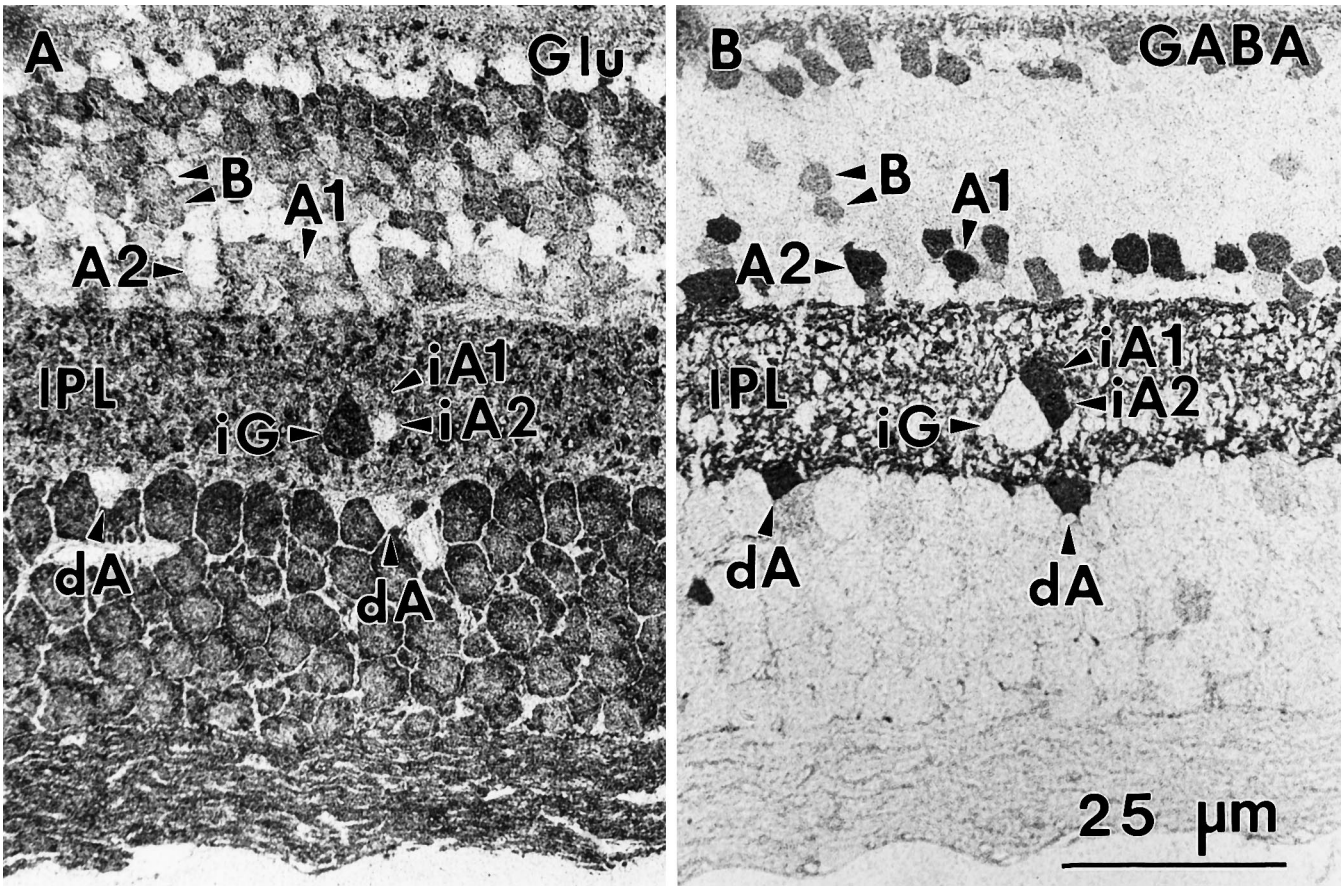

Figure 7. Serial sections (sample 571) 1–3 mm from the fovea labeled for glutamate (*A*) and GABA (*B*). Two examples are given of the differences in glutamate precursor pools in conventional γ^+ amacrine cells (*A1* and *A2*) and interstitial γ^+ amacrine cells (*iA1* and *iA2*). Two γ^+ bipolar cells are also indicated. Abbreviations defined in legend to Figure 1.

ganglion cells and their axons segregate from all other classes because they display a range of red hues. Further indications of subtle differences between rods and cones occur in the outer nuclear layer and among bipolar cell subsets in the inner nuclear layer. Ganglion cells, however, do not clearly segregate from bipolar cells. GABA signals (blue hues) are present in horizontal cells and amacrine cells and in displaced amacrine cells in the ganglion cell layer and the inner plexiform layer proper. Some cells display magenta hues, illustrating concordance of glutamate and GABA signals, but there is no simple visual way to subset γ^+ cells. There is no pure green glycine signal, because glycine always colocalizes with significant glutamate signals (yellow hues) in most presumed glycinergic amacrine cells. Note the yellow hues in a subpopulation of bipolar-like cells identifying the glycine-rich presumptive bipolar cell group and instances of purple hues identifying a presumed bipolar cell subset with weak GABA signals. Amacrine cells containing high levels of both GABA and glycine are illustrated later (see "Amino acid patterns in midperipheral and far-peripheral retina").

*Figure 8*B, *τQE*→rgb *mapping*

The inclusion of taurine and glutamine signals demonstrates that most bipolar cells and photoreceptors are biochemically distinct from ganglion cells. The brighter cyan hues identify ganglion cells, and darker greens and reds index amacrine cells that display strong glutamate signals. The taurine-rich Müller's cells show a unique orange band above the amacrine cell layer that clearly denotes a separate biochemical class. Moreover, the fine black bands coursing through the ganglion cell layer in Figure 8*A* are now shown to be glutamine- and taurine-rich processes of Müller's cells; however, identification of presumptive bipolar or amacrine cell subsets remains nearly impossible.

Pattern recognition of amino acid signatures

The *rgb* images reveal strong biochemical diversity and constitute qualitative evidence for subpopulations. Each triplet, however, provides limited class differentiation, and the bewildering galaxy of hues challenges visual analysis. Conversely, pattern recognition extracts quantitative signal correlations from all amino acids in all cell groups and reclassifies the image as a theme map of statistical entities. The outcome of K-means classification of the retina shown in Figure 8 is summarized in Figure 9 and is representative of primate retina at 1–3 mm eccentricity. The 15 map colors encode the different cell populations as separable theme classes. Similar analyses were performed at five retinal loci in a sample that extended >500 μm linear extent for each and contained several hundred to several thousand somas. Sixteen separable theme classes were defined, and three classes were further divisible into *significant* but not *separable* subsets on biochemical grounds (Table 1).

The comprehensive theme map shows that cone photoreceptors, the Henle's fibers, and rod nuclei comprise class E1 cells in the outer nuclear layer. Rods, however, form a morphological class with slightly higher glutamate signals than cones, and al-

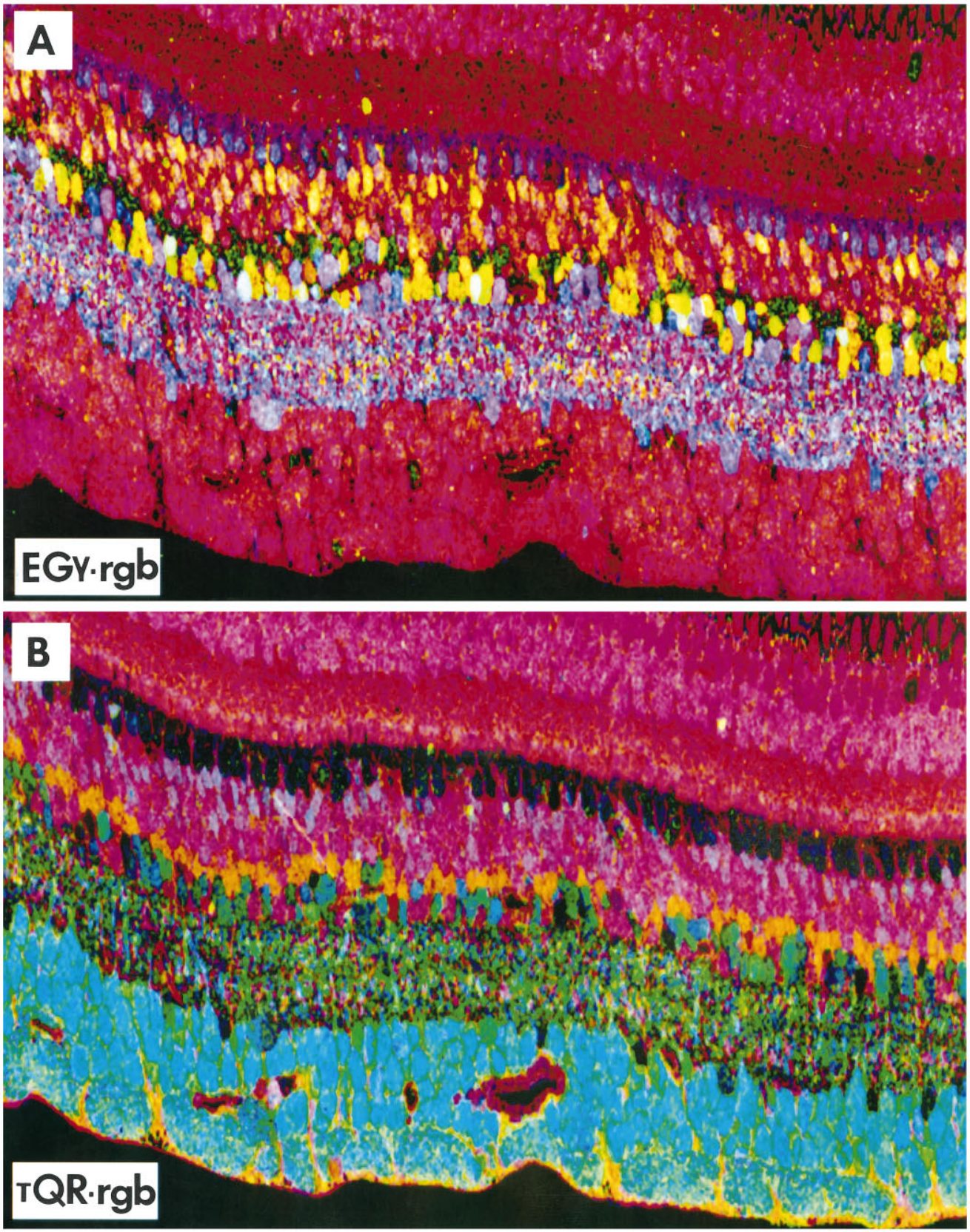

Figure 8. Amino acid→*rgb* mappings from registered serial 250 nm sections of primate retina (sample 571) 1–3 mm from the fovea. *A*, EGγ→*rgb*; *B*, τQE→*rgb*. See text for discussion.

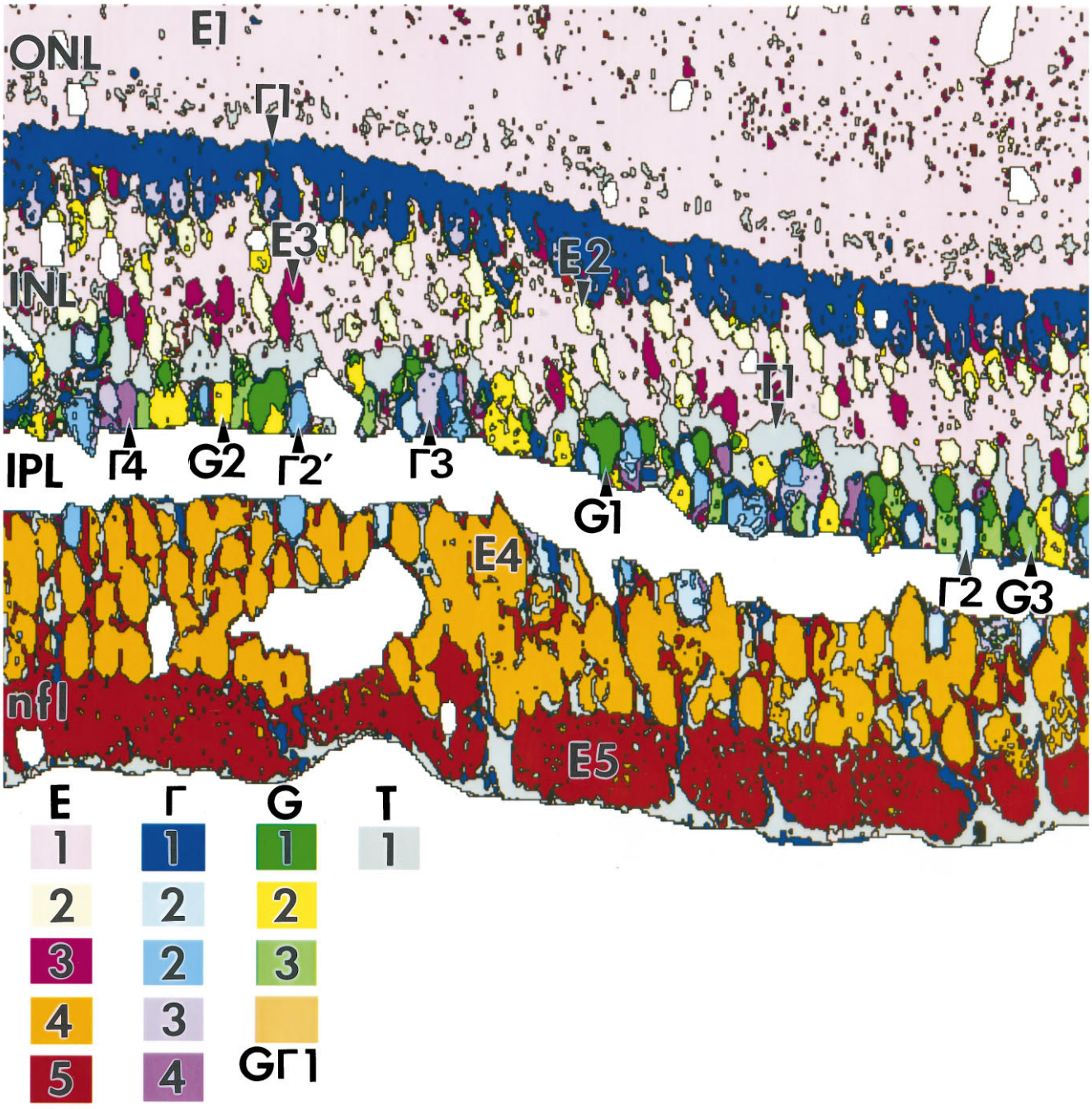

Figure 9. Theme map of the primate retina (sample 571) 1–3 mm from the fovea. The map color codes used in all theme maps are shown at *bottom*. Each cell class is defined by K-means clustering and exhibits $D^T \geq 1.9$, except where noted otherwise (see Materials and Methods). The inner plexiform layer (*IPL*) has been masked off and collapsed in this and other theme maps, because the resolution of serial 250 nm section pattern recognition is insufficient to classify processes in the IPL. *White areas* in the retina proper correspond to blood vessels. Holes in a single section or other artifacts were excluded from analysis. Abbreviations defined in legend to Figure 1.

though insufficient to define rods as a separable biochemical group, the difference is statistically significant and warrants identifying class **E1′** as a subset containing cones. Similar to those in the goldfish retina, many bipolar cells and photoreceptors share the same **E1** signature, but the primate retina shows more complexity in that both type **E1** and **E1′** signatures occur in the bipolar cell cohort (not shown in the theme map). We do not know whether this indicates simple biological variability within some or all bipolar cells in the **E1** class or whether two functional types of bipolar cells are being exposed. As a group, however, the **E1** cohort is separable from all other retinal neurons. Glycine-rich **E2** bipolar cells are often located distally in the inner nuclear layer just below the horizontal cells, with **E1** bipolar cells in mid-inner nuclear layer and weakly GABA-immunoreactive **E3** bipolar cells closer to Müller's cells. The amacrine cell layer is dominated by **G** and Γ theme groups, and class **E** groups are largely excluded therefrom, except in the very foveal pit and sometimes in the far periphery. Glycine-rich amacrine cells are separable into three

Table 1. Theme classes, primary signals, cell types, and signal separabilities in the macaque retina

Theme class	Key amino acids	Probable cell types	Separability
E1	Glutamate	Rods and BCs	All but **E1′**
E1′	Glutamate	Cones and BCs	All but **E1**
E2	Glutamate	G^+ ON-cone BCs	All but **E2′**
E2′	Glutamate	G^+ ON-cone BCs	All but **E2**
E3	Glutamate	γ^+ BCs	Complete
E4	Glutamate	Most GCs	Complete
E5	Glutamate	τ^+ GC subset	Complete
E6	Glutamate	γ^+ GC subset	Complete
G1	Glycine	ACs	Complete
G2	Glycine	AII ACs	Complete
G3	Glycine	ACs	Complete
GΓ1	Glycine/GABA	ACs	Complete
Γ1	GABA	Central HCs	Complete
Γ2	GABA	ACs	All but **Γ2′**
Γ2′	GABA	ACs	All but **Γ2**
Γ3	GABA	ACs	Complete
Γ4	GABA	ACs	Complete
T1	Taurine	MCs	Complete
X1	?	Peripheral HCs/ACs	Complete

BC, Bipolar cell; GC, ganglion cell; AC, amacrine cell; HC, horizontal cell; MC, Müller's cell.

distinct populations (**G1, G2, G3**), and GABA-rich amacrine cells form a similarly complex population (**Γ2**, **Γ2′**, **Γ3**, **Γ4**). Müller's cell form a distinct band of somas just distal to the amacrine cell layer, constituting the T1 theme group. Thus a distinct laminar neurochemical order appears to be present in the central inner nuclear layer of the primate retina: distally→proximally, **Γ1** horizontal cells, **E2** bipolar cells, **E1** bipolar cells, **E3** bipolar cells, **T1** Müller's cells, and the amacrine cell cohort, very similar to that described in the chicken retina (Kalloniatis and Fletcher, 1993). In fact one can distinguish legitimate "amacrine cell" and "Müller's cell" layers on quantitative grounds. In central retina >0.5-3.0 mm (excluding the variable region near the foveal floor), the amacrine cell layer bordering the inner plexiform layer is comprised of 40% class Γ cells, 40% class **G** cells, 15% class **E** cells, and 5% class **T1** (Müller's) cells. Just distal to the amacrine cell layer, the Müller's cell layer is composed of 10% class Γ cells, 5% class **G** cells, 30% class **E** cells and 55% class **T1** (Müller's) cells. Within the ganglion cell layer, presumed displaced amacrine cells display multiple Γ theme classes, and these cells rarely occur outside the first row of cells in the ganglion cell layer. Most ganglion cells have the **E4** signature, but occasional taurine-rich **E5** ganglion cells exist. The nerve fiber layer also displays the **E5** signature, and this is attributable to the fact that the fine τ^- but strongly E^+ axons are all ensheathed by fine lamellae of E^-, but τ^+ glial cells on a scale smaller than the spatial resolution of our pattern recognition algorithms. Thus both axons and sheaths are grouped into a single class indistinguishable from the truly τ^+ and E^+ ganglion cell somas. The biochemical features of these and other theme classes will be elaborated below (see "Visualizing signatures").

Pattern recognition in the fovea proper

Figure 10 shows serial sections from a primate fovea (M328) labeled for glutamate, GABA, taurine, glycine, aspartate, and glutamine, followed by a complete theme map established by pattern recognition analysis (Fig. 11). The amino acid labeling pattern in central fovea displays many of the features noted earlier, with some interesting exceptions. Amino acid labeling at the foveolar edge appears in "disarray," with somas failing to show the neurochemical order present 50–100 μm from the foveal pit. Bipolar cells, ganglion cells, and amacrine cells all occur on the edge of the foveal pit, with both GABA and some glycine signals extending into the foveal floor (also see Hendrickson et al., 1988; Grünert et al., 1993). The glycine-rich **E2** bipolar cell class is prominent in the fovea and along with the **G2** amacrine cell class extends to within 100 μm of the foveal floor. If the glycine signal found in bipolar cells is attributable to amacrine cell–bipolar cell gap junctional coupling (Cohen and Sterling, 1986), then this coupling clearly extends to the foveal edge where both **G2** and **E2** signatures coexist. It is also possible that the glycine signal of **E2** cells is somehow independent of coupling with **G2** cells. The laminar neurochemical order within the inner nuclear layer is clearly initiated within 100 μm of the foveolar edge and is well established by 1 mm eccentricity and beyond. Furthermore, **E5** ganglion cells exist in the fovea proper, and their low numbers imply that **E4** cells represent the bulk or perhaps all of the midget ganglion cell population. Although the foveal horizontal cells in this retina have a distinct γ^+ signal, it is quite faint and consistent with previous observations that primate horizontal cell GABA signals are volatile.

Amino acid patterns in midperipheral and far-peripheral retina

The general neurochemical order within the inner nuclear layer begins to disappear in midperipheral and far-peripheral retina as overall cell numbers decline, and there are significant changes in certain signatures and theme classes. In the midperipheral to far-peripheral retina, **E1** and **E2** bipolar cells are both present but clearly intermixed rather than stratified (Fig. 12). The GABA-immunoreactive **E3** bipolar cell theme class absolutely disappears, and all horizontal cells are GABA immunonegative. We also find that 8% of the amacrine cells in the midperiphery in these samples lack GABA or glycine immunoreactivity. Because bipolar cells sometimes occur in the amacrine cell layer in peripheral retina, we verified that these "empty" cells do not belong to a glutamate theme group (**E1**) but are rather classified by the clustering algorithm as a group that includes peripheral horizontal cells. These amacrine cells are indistinguishable from peripheral horizontal cells and both have been assigned provisionally to class **X1**, a class with no known dominant amino acid signal. Their strongest signal is glutamate, but even that is rather weak.

Peripheral **G2** amacrine cells are almost always found at the border of the inner plexiform layer, display a thick proximal dendrite, and are characterized further by a strong taurine signal (Fig. 12). These same features have been attributed previously to the AII amacrine cell (Kolb and Nelson, 1983; Hendrickson et al., 1988; Vaney, 1990; Wässle et al., 1995). It has now been shown that like primate AII amacrine cells (Wässle et al., 1995), **G2** amacrine cells in macaque retina are calretinin immunoreactive (Zhang et al., 1996). Thus it seems likely that AII amacrine cells are **G2** amacrine cells and *vice versa*. A further alteration of significance in peripheral retina is an apparent increase in the frequency of **GΓ1** amacrine cells. This observation will have to be quantitatively tested by comprehensive horizontal section analyses of all retinal layers at all eccentricities, but this distinctive group is seen less frequently in central retina. Such cells are among the rarest amacrine cells in the goldfish retina. Approximately 50% of

the retinal volume in the far periphery can be assigned to Müller's cells as neuronal numbers decline. Within the ganglion cell layer, nearly half of the somas display GABA signals, and many may be GABAergic amacrine cells, consistent with known density changes of amacrine cells in the ganglion cell layer of the monkey retina (Wässle et al., 1990). Some are certain to be γ^+ ganglion cells, however, because many mammals have bona fide ganglion cells with some GABA signals (identified as **E6** in Fig. 12), and γ^+ axons are definitely present in the optic nerve (Wilson et al., 1996).

Visualizing signatures

The penultimate objective of pattern recognition is extracting a fingerprint or definitive signature from a class. Each theme class is characterized by six-dimensional means, variances, and covariances. To simplify this complex signature, we can compare signatures where cellular amino acid contents are plotted as histograms in probability density distribution format (Fig. 13): a univariate signature matrix. Although we lack biochemical data from homogenized primate retinas to absolutely calibrate these distributions as we have done for goldfish retina, it is nevertheless clear that the signal values obtained here scale to the same ranges of molar concentrations (≈0.1-20.0 mM). It is important to understand that classification by pattern recognition is independent of concentration units or signal scaling (Marc et al., 1995): classes exist by virtue of their relative signal positions in N-space. In any vertical column of the matrix in Figure 13, signal peaks positioned at the left and right borders of an abscissa, respectively, denote lower and higher intracellular concentrations. As an example, we may compare glycine values across all theme classes merely by reading down a column. It is evident that some sets of cells have higher glycine signals and are thus named class **G** cells: **G1, G2, G3** and **GΓ1**. Within that group it is relatively simple to distinguish **G1** cells from **GΓ1** amacrine cells based on the additional signal of GABA content. It is rather difficult at first glance, however, to determine how one might differentiate the glycine-rich **G1** and **G2** classes until one compares their taurine contents. Recognizing further differentiations by pairwise comparisons across six sets of amino acids and hundreds to thousands of cells is effectively impossible, because one cannot visually abstract such data to test hypotheses. For example, the problem of determining key signature differences is even more complex if one attempts to determine the basis of separating classes **G1** and **G3** by inspection of univariate histograms. In truth, no univariate signal can adequately separate these groups. Rather, they are separate classes partially because their respective glycine and taurine signals segregate in bivariate space (Fig. 14*A*). Similarly, the glycine signal of the **G2** amacrine cell population overlaps substantially with the glycine signal of **E2** bipolar cells, so that any one amino acid is insufficient to uniquely specify the two cohorts. It is through pattern recognition, taking into account all six amino acids, that we can classify **E2** and **G2** as unique groups with $D^T > 1.9$. As noted previously, it is possible to recognize an **E2′** subclass in the **E2** cohort by pattern recognition, which differs primarily on the basis of glycine content, although it is not separable. This is reflected in the broad spectrum of signals in the **E2** univariate glycine histogram.

GABA-dominated theme classes can easily be distinguished from the other major forms but classifying them further requires a full pattern recognition analysis. The **Γ1** horizontal cell class is distinctive in that the GABA signal is weak, and the class has lower glutamine values than other members of the Γ cohort. The dominant amacrine cell class is group **Γ2**, with smaller numbers of cells comprising groups **Γ3** and **Γ4**. Quantitative horizontal section analysis will be required to fully resolve the population numbers. **Γ2** cells are distinguished by a virtual absence of any taurine signals but contain a fairly strong glutamate signal. At the other extreme, **Γ4** cells have the strongest taurine signals of any γ^+ amacrine cell yet have very weak glutamate signals (Fig. 13). Class **Γ3** cells constitute an intermediate but separable variety. It is possible, however, to distinguish an additional significant population that is separable from all other classes except **Γ2**, and we denote it **Γ2′**. The functional identities of these biochemical types are currently unknown.

The third and most complex class contains the E^+ photoreceptors, bipolar cells, and ganglion cells. Some broad separations can be made based on relatively simple signal separations. For example, all bipolar cells and photoreceptors (**E1**, **E2**, **E3**) are always separable from all ganglion cells (**E4**, **E5**, **E6**), based largely on the low taurine and/or high glutamine signals in the latter. Within the photoreceptor/bipolar cell cohort, **E2** and **E3** bipolar cells separate distinctively because of elevated glycine and GABA signals, respectively. Significant biochemical subclasses seem to exist for both **E1** cells, as indicated previously with class **E1** proper representing rods and roughly half of the **E1** bipolar cell cohort and **E1′** containing cones and the remaining class **E1** bipolar cells (see Table 1). The **E2** class similarly shows significant subdivision of cells into **E2** and **E2′**, as noted above. Within the ganglion cell cohort, **E4** cells dominate the central retina and differ from both **E5** and **E6** cells in having no measurable taurine signal. A small population of τ^+ ganglion cells may denote a second functional class, which appears mingled with **E4** cells within 150 μm of the foveal floor. Conversely, a set of $\tau^+\gamma^+$ class **E6** cells is quite infrequent in central retina but very common in the periphery and may represent the primate homolog of presumed GABAergic ganglion cell described in other mammals (Yu et al., 1988).

Bivariate distributions

Bivariate and trivariate probability density distributions allow some richer biochemical inferences. Figure 14 displays one of 15 possible bivariate and one of 20 possible trivariate comparisons for the six amino acids. For example, Figure 14*A* reflects the distributions of signals in **G1**, **G2**, and **G3** amacrine cells in glycine–taurine space and displays a particularly powerful example of how signal covariance rather than simple differences in means can lead to class separations. The overlap of the univariate distributions for either glycine or taurine alone renders the nominal **G1** and **G3** classes inseparable, and no other amino acid signal offers any clue as to biochemical differences. Bivariate plots, however, show that glycine and taurine signals covary in an orderly way within each class. This is reflected in the elliptical shapes of the 2 SD bounds, with a negative correlation between glycine and taurine content and effectively no significant overlap between classes **G1** and **G3**. For reference, the highly separated **G2** class shows a radially symmetric 2 SD bound, showing that the glycine–taurine correlation is not an intrinsic feature of all cells. Indeed, only pattern recognition can extract such relations: covariance is not detectable on visual examination of cells.

Even more complex associations, however, occur *across* classes that are not visually obvious until higher-order visualization is used. Figure 14*B* reflects the associations among glutamate, glutamine, and aspartate for most neuronal classes. Aspartate and glutamine are potential glutamate precursors and show monotonic correlations with glutamate levels across all classes. The cells

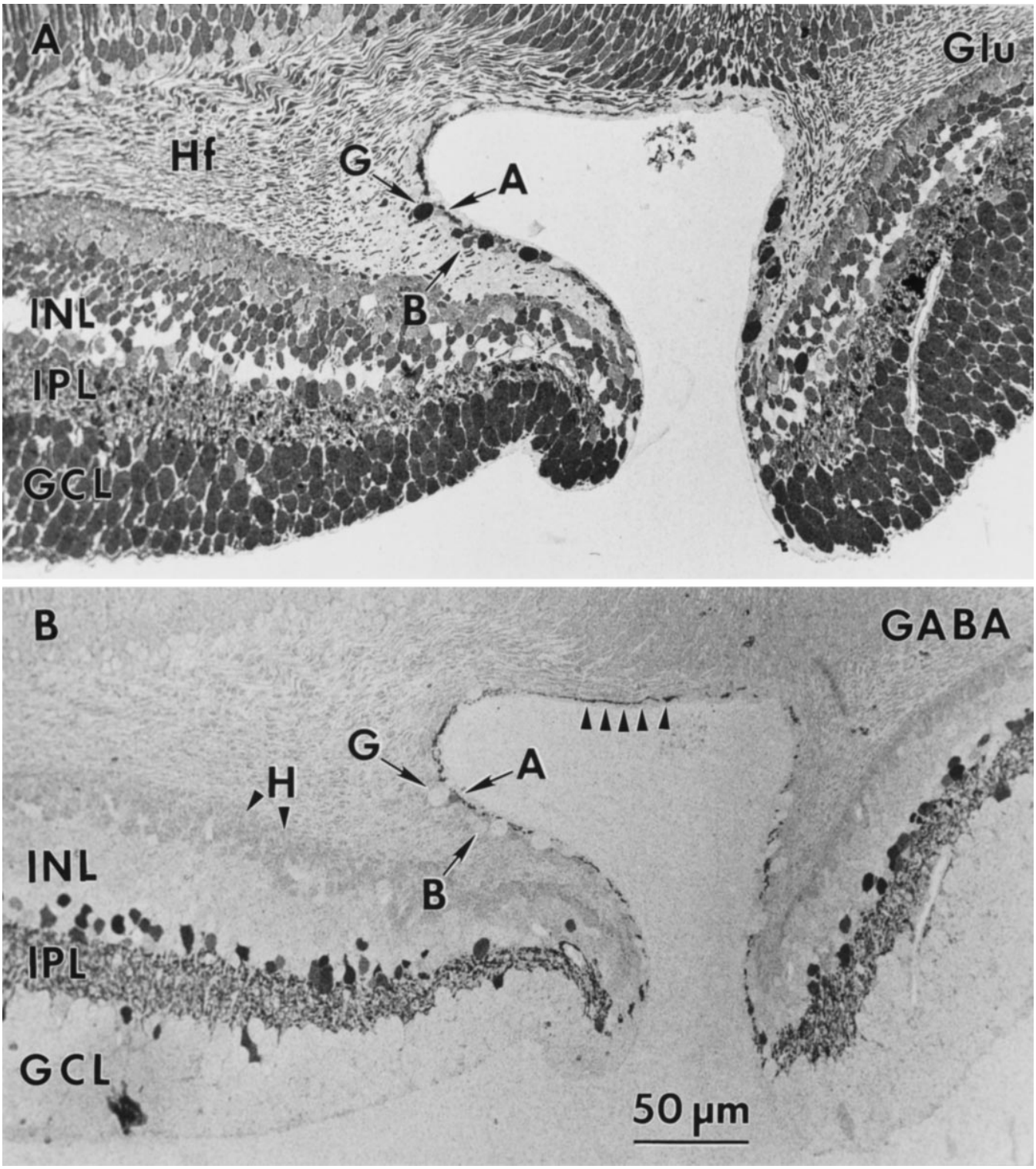

Figure 10. Foveal serial sections (sample M328) labeled for glutamate (*A*), GABA (*B*), taurine (*C*), glycine (*D*), aspartate (*E*), and glutamine (*F*). A **G** Γ**1** amacrine cell (*A* with *arrow*), an **E4** ganglion cell (*G* with *arrow*), and an **E1** bipolar cell (*B* with *arrow*) on the foveal edge are indicated. Note the disarray of the immunoreactivity in the inner nuclear layer (*INL*) near the foveal edge and the GABA processes in the foveal floor (identified by *arrowheads* in *B*). *Hf*, Henle's fibers. Other abbreviations defined in legend to Figure 1.

Figure continues.

with the highest glutamate contents are also those with the highest glutamine and aspartate levels, indicating some fundamental coherence in metabolic relations. Because it is difficult to gauge position and overlap in three-space, bivariate plots of the 2 SD bounds offer simpler views of the relative signal strengths and dispersions of key classes in the comparison, e.g., glutamate versus aspartate for class **E1–E4** cells and **T1** Müller's cells (Fig. 15). Again, the ganglion cell theme class **E4** shows the highest levels of

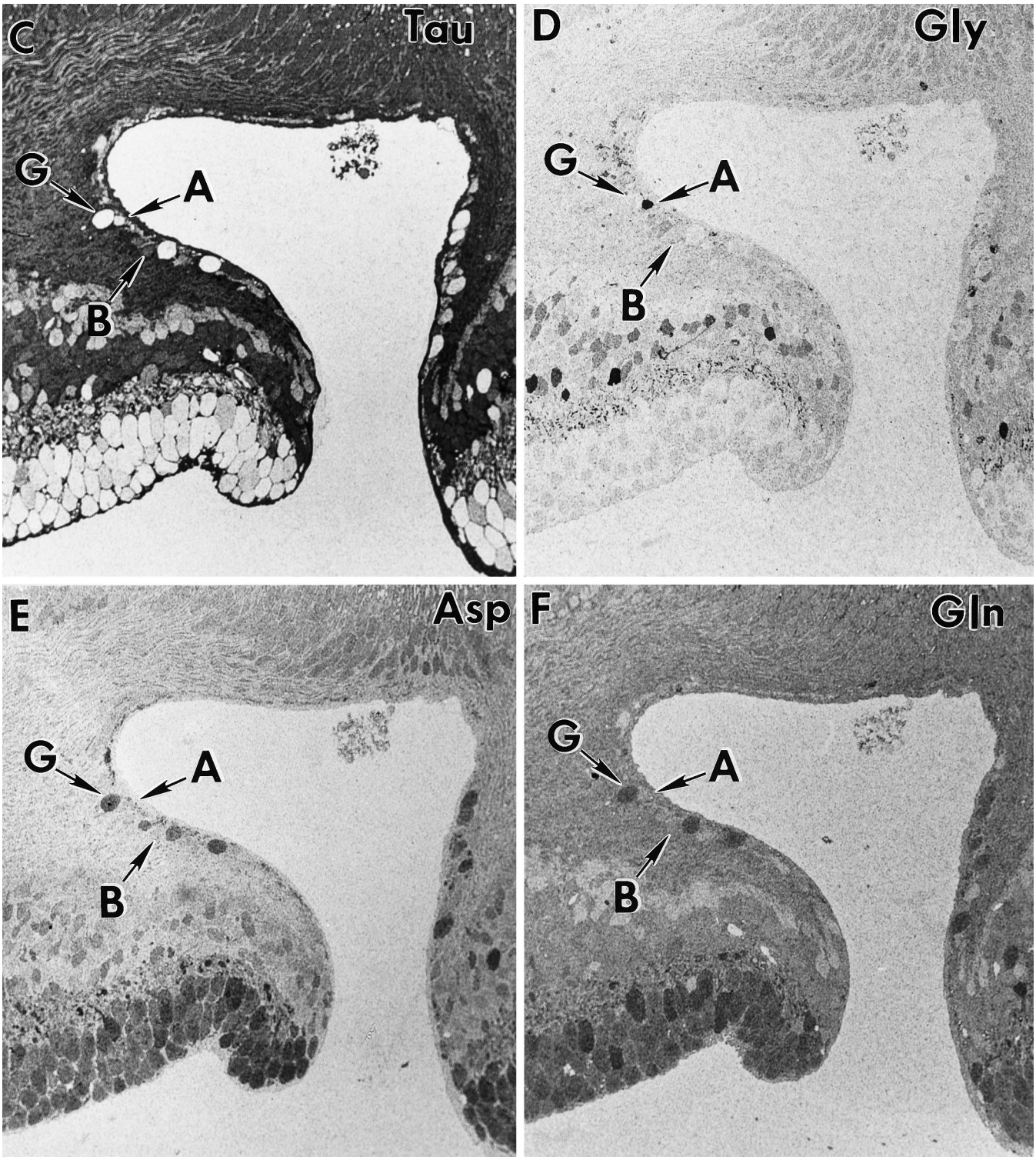

Figure 10 continued.

glutamate and aspartate, in agreement with photomicrographs (Figs. 1, 4, 5) and the signature matrix. Other glutamate-dominated theme classes also fall on the diagonal, although at different locations, indicating a reduced amino acid content compared with **E4**. This monotonic association among potential precursors glutamine, aspartate, and glutamate holds for almost all cell classes. One notable exception to this is the **T1** glial signature where the distribution falls outside the diagonal; glutamine levels are very high in Müller's cells because of their exclusive content of glutamine synthetase. Although these findings suggest an obvious biochemical linkage among glutamate, aspartate, and glutamine, this is not a universal feature of vertebrate retinas. Marc et al. (1995) did not find such a simple association in the goldfish, and we have found a poor correlation in the rat retina (M. Kalloniatis, unpublished data).

Finally, large groupings of cell classes with separable signatures can be seen to form other biochemical hierarchies. Glycine levels have a rough tristratification in bivariate space (Fig. 16), which

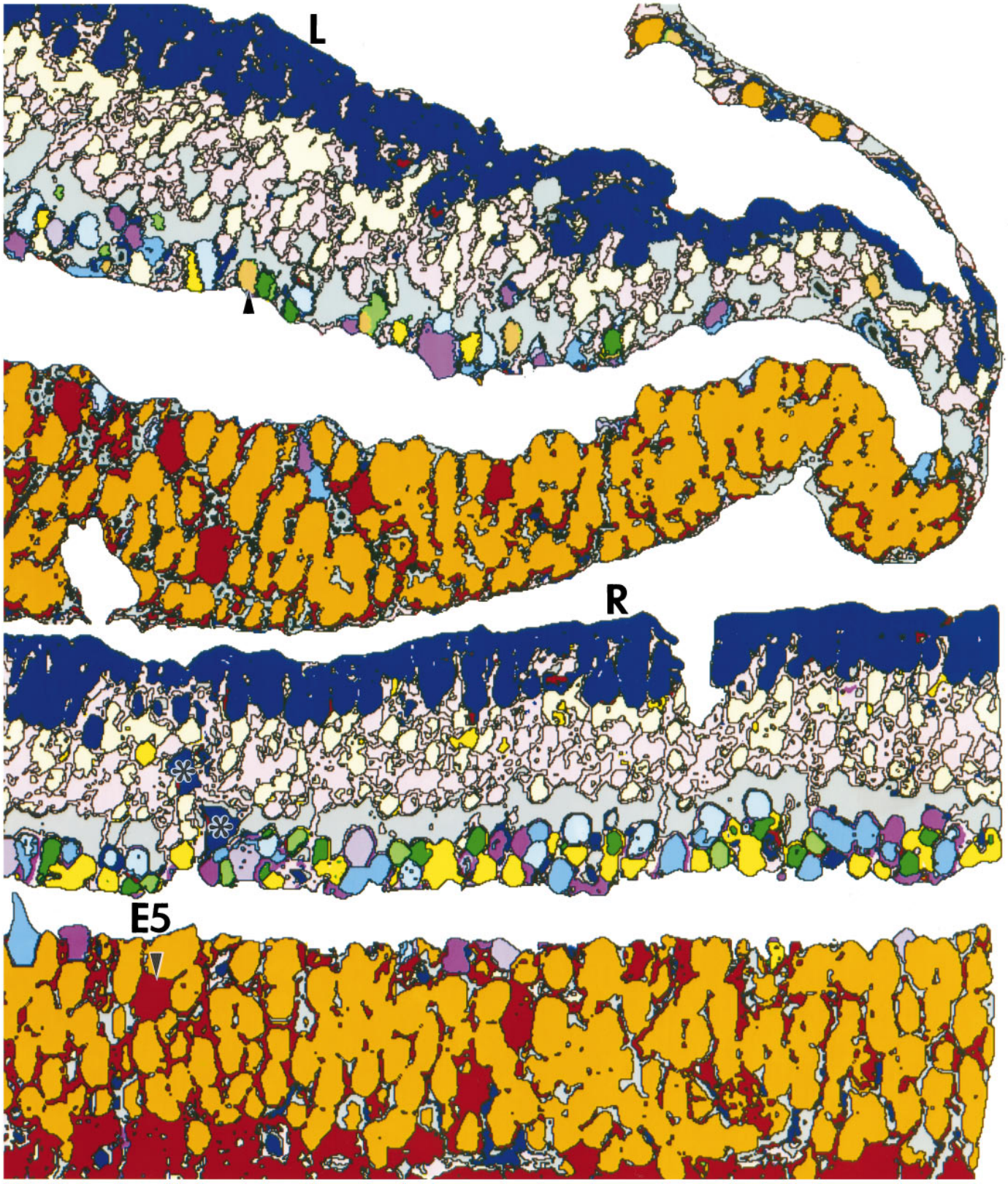

Figure 11. Theme map (sample M328) of primate fovea (*L*) and at an eccentricity of 1 mm (*R*). Note the *pale brown* **G Γ1** amacrine cells in the amacrine cell layer (one indicated by an *arrowhead*), the abundance of **E5** ganglion cells, and what may be displaced horizontal cell somas (*asterisks*). The photoreceptor layer has been removed for clarity, and the inner plexiform layer has been masked as in Figure 9.

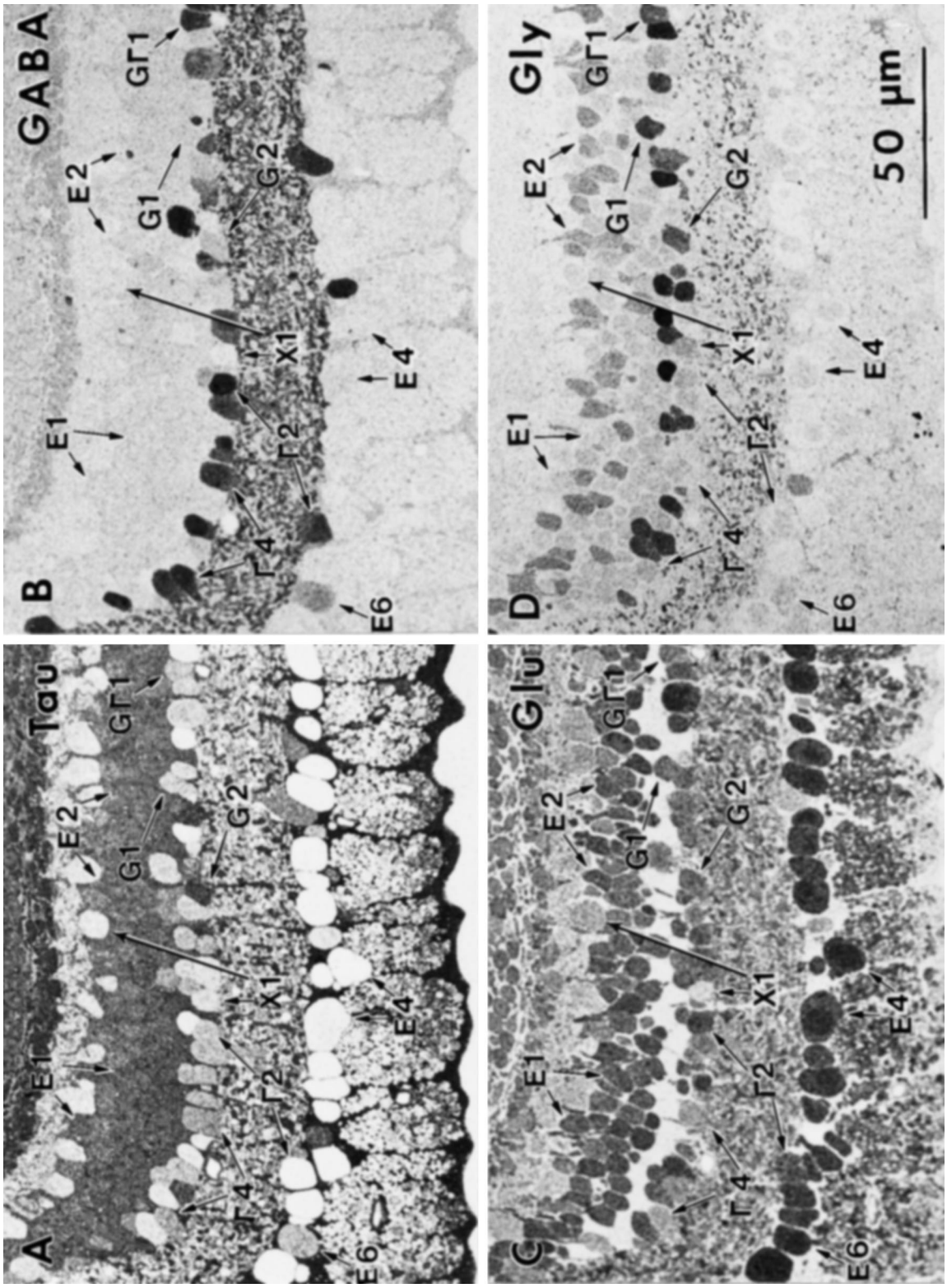

Figure 12. Serial sections of midperipheral primate retina (sample M328) at 4–6 mm eccentricity, consecutively labeled for taurine (*A*), GABA (*B*), glutamate (*C*), and glycine (*D*). Several theme groups based on pattern recognition classification are indicated, including **X1** (*X1*) cells with their "null" signatures, **G Γ1** amacrine cells (*GΓ1*), **Γ2** (*G2*), and **Γ4** (*Γ4*) amacrine cells to highlight the distinctively higher glutamate signals of **Γ2** cells (Γ2), G^+ **E2** (*E2*) and G^- **E1** (*E1*) bipolar cells, τ^+ **G2** and τ^- **G1** amacrine cells, conventional **E4** (*E4*) ganglion cells, and a weakly γ^+ **E6** (*E6*) ganglion cell. A **GΓ1** amacrine cell is also indicated.

indicates some fundamental divisions between likely transmitter and basal glycine pools (high glycine **G1**, **G2**, **G3** cells vs low glycine **E1**, **E3**, **E4** cells, respectively). Although we have not focused on absolute calibrations in this report, the low glycine signals in **E4** ganglion cells and class **E1** and **E3** cells likely represent 100–400 μM levels based on direct comparison with calibrated data in Marc et al. (1995). Clearly, **G1** amacrine cells have the highest glycine contents of all neurons (likely >10 mM), whereas **G2** and **G3** cells show low millimolar signals. Certain presumably nonglycinergic cells such as **E2** bipolar cells do overlap into what we believe is the bona fide "neurotransmitter" level of glycine. Our current interpretation is that all **E2** cells represent various types of ON-center cone bipolar cells coupled to **G2** (i.e., AII) amacrine cells by gap junctions. If so, the presumed primary

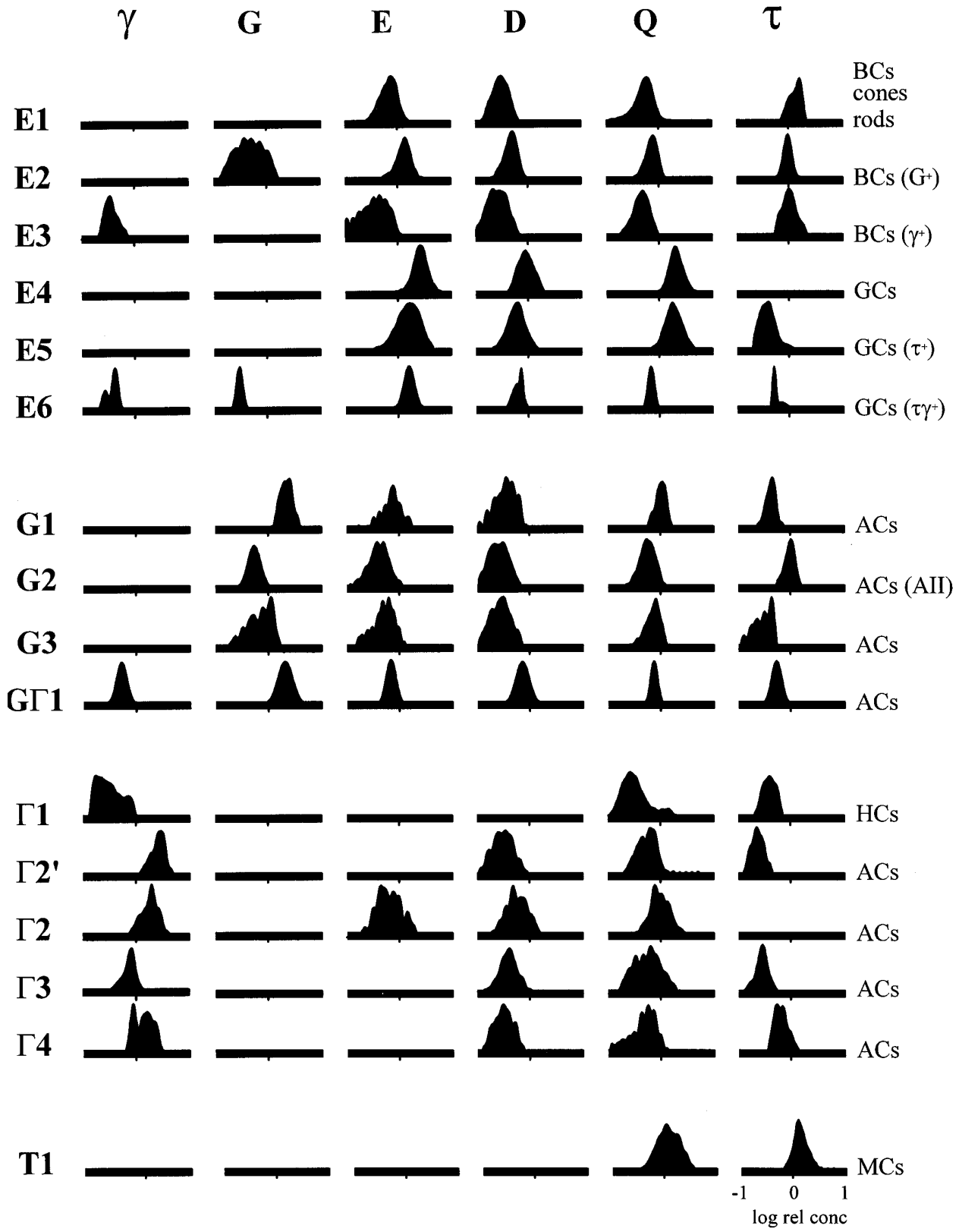

Figure 13. The signature matrix for the central primate retina. The *left column* identifies the theme class, and the *right column* identifies the cell class. Amino acids are grouped in vertical columns: GABA (γ), glycine (*G*), glutamate (*E*), aspartate (*D*), glutamine (*Q*), and taurine (τ). Each column demonstrates the distribution of a single amino acid across all theme classes, and each row is the univariate signature for each class. All probability density distributions are amplitude-normalized; the ordinate denotes the relative spectral density along an abscissa of increasing relative log amino acid concentration. Histograms were FFT-filtered to yield a resolution of ~16 Hz, i.e., 16 unique concentration levels in 0.125 log unit steps in discrete terms. Signals with means ≤ −1 log units relative concentration are not included. *BC*, Bipolar cell; *GC*, ganglion cell; *AC*, amacrine cell; *HC*, horizontal cell; *MC*; Müller's cell.

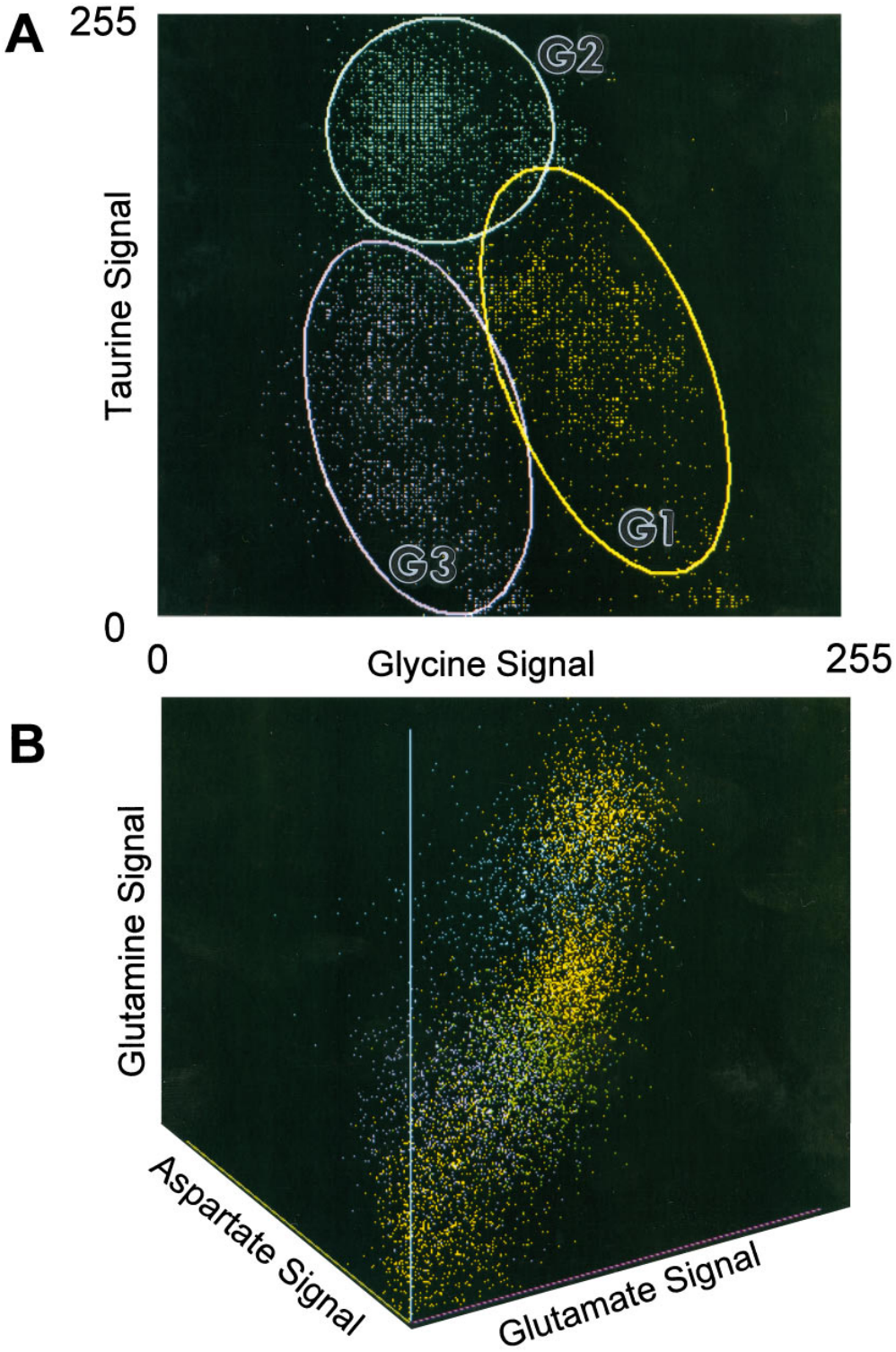

Figure 14. Bivariate and trivariate scatterplots of theme class amino acid signals. *A*, Glycine versus taurine distribution for the **G** theme class, demonstrating the nearly univariate separation of **G2** (*cyan*) cells from **G1** (*yellow*) and **G3** (*purple*) cells. Conversely, no univariate signal statistically separates **G1** and **G3** cells, but they do separate in N-space because of signal covariance within a class. The points are subsets of all the data points from **G** cells in retina at 1–3 mm eccentricity, and the ellipses represent the 2 SD bounds of the distributions. *B*, The coherent distribution of glutamate, aspartate, and glutamine signals from various **E** and **G** cells. Sample points from each theme class are denoted as various colors (**E1′**, **E2**, and **E4** cells as *various yellows*; **E1** and **E2′** cells as *blues*; **E3** cells as *magenta*; and **G1** cells as *green*). Although it is not possible to sort out the groupings, the important point is the apparent monotonic relationships along the glutamate/glutamine and glutamate/aspartate dimensions. A detailed dissection of some of these groups is shown in Figures 15 and 16.

synthetic source of glycine would be **G2** amacrine cells, and they would be responsible for adventitious loading of the entire **E2** cohort with glycine. Similarly, the **E2** bipolar cells would be the likely source of reciprocal taurine signals leaking into **G2** amacrine cells; however, **E2** bipolar cells sometimes display higher levels of glycine than the apparent source **G2** population (Pourcho and Goebel, 1987). Although this is not explicable by simple diffusion, many possible glycine sources and sinks exist for each cell, and unexpected dynamic equilibria can arise in such cases. It is also possible that **E2** cells have a mechanism for concentrating intracellular glycine that is completely independent of coupling with **G2** amacrine cells. Although separable from **G2** cells in N-variate space, no single bivariate space shows complete **G2**/**E2** separability, further emphasizing that the power of pattern recognition is extracting unique populations from complex signal spaces. The accuracy of the **G2** grouping is further validated by the recent demonstration that all calretinin-immunoreactive amacrine cells have the **G2** signature (Zhang et al., 1996), and all

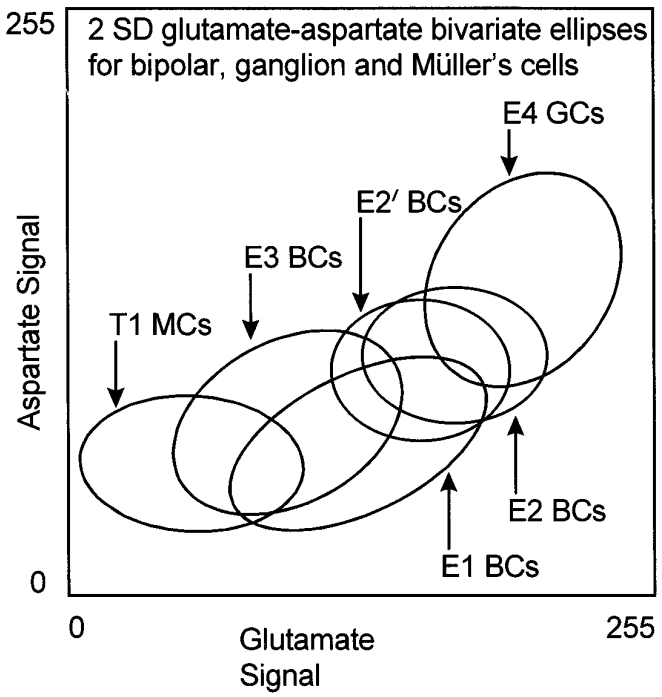

Figure 15. Bivariate single class 2 SD ellipses demonstrating the monotonic relationship between glutamate and aspartate levels across type **E** cells. Note the downward displacement of the **E1** bipolar cells (and photoreceptors) from the trend and the upward displacement of **T1** Müller's cells to slightly higher aspartate levels than expected based on their low basal glutamate content. Abbreviations defined in legend to Figure 13.

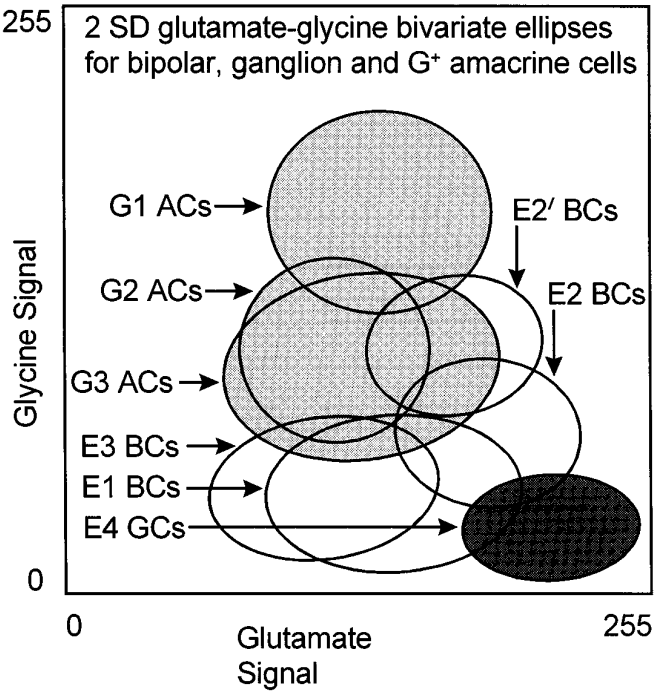

Figure 16. Bivariate single class 2 SD ellipses of glutamate and glycine signals across type **E** and **G** cells. In particular, note the stratification of cells into low glycine and high glycine regimes and the separations of **E2** and **E2′** bipolar cells into two modes. Abbreviations defined in legend to Figure 13.

strongly calretinin-immunoreactive conventionally placed amacrine cells seem to be AII amacrine cells (Wässle et al., 1995).

DISCUSSION

Pattern recognition classifies virtually all retinal space

As illustrated in Figures 8, 9, and 11, and summarized in Table 1, all neuronal space in the central primate retina can be parsed into separable classes enriched in the amino acids (glutamate, GABA, or glycine) that subserve most fast neurotransmission in retina and CNS (Sarthy et al., 1986; Yazulla, 1986; Ehinger et al., 1988; Hendrickson et al., 1988; Montero and Wenthold, 1989; Grünert and Wässle, 1990; Marc et al., 1990, 1995; Massey, 1990; Muller and Marc, 1990; Kalloniatis and Fletcher, 1993). Taurine-rich glia and vascular cells comprise the remaining space. We have no evidence for "empty" or unclassifiable cells in central retina, but class **X1** cells with "null" signatures occur in peripheral retina. In summary, pattern recognition of amino acid signals identifies two types of photoreceptors (**E1** rods and **E1′** cones), four bipolar cell types, three ganglion cell types, four G^+ amacrine cell types, one horizontal cell type, and four γ^+ amacrine cell types.

Are theme classes functional classes?

Simply because a cell has an unusual signature does not necessarily imply that it constitutes a physiologically or morphologically distinct class. It is theoretically possible that long-lasting metabolic changes in a subset of cells can be produced by pathological or other conditions. Our analyses, however, provide strong evidence that most signature types associated with separable theme classes represent functional classes in the most generic sense. Commonly recognized types such as horizontal cells, Müller's cells, most ganglion cells, etc., demonstrate biochemical separability and homogeneity. Figure 1*B* illustrates this well for GABA signals. Although horizontal cell GABA signals are weaker than most amacrine cell GABA signals, the signals are extremely homogeneous across all horizontal cells. As we improve morphological resolution in our pattern recognition methods, other homogenous biochemical classes clearly have homogeneous anatomical equivalents, such as **G2** and AII amacrine cells. The preponderance of **E4** ganglion cells in the fovea and central retina implies that this group likely includes midget ganglion cells. **E5** cells may represent additional ganglion cell types that approach the foveal floor, but we lack data to support a functional classification. The **Γ2**, **Γ2′**, **Γ3**, and **Γ4** amacrine cell cohorts are too complex to subdivide at present, but we have evidence that some **Γ2** cells in the rabbit retina represent the starburst amacrine cell cohort (Marc, 1996). We believe that most theme classes will eventually map directly to classical cell types.

What does signature heterogeneity mean?

Patterns of amino acid signals are stable on the whole, but absolute levels may vary within a retina and between specimens; however, although the horizontal cell GABA signal is variable in the monkey retina, $GABA_A$ receptors have been localized in the outer plexiform layer (Grünert et al., 1993), and horizontal cells show GAD_{65} immunoreactivity (Vardi and Sterling, 1994; Vardi et al., 1994). This presents a serious problem for interpreting the *absence* of GABA immunoreactivity in many mammalian retinas. How much GABA is required to "run" a horizontal cell synapse? Why is horizontal cell GABA content capricious? It is not clear that cytopathology can be invoked as an explanation, because foveal horizontal cells with weak or no GABA immunoreactivity can occur even when no central amacrine cells show any GABA

losses. These observations imply that horizontal cells containing <100 μM GABA may still function as GABAergic neurons *in vivo*, which would challenge the sensitivity of immunochemical analysis. Consistent with this speculation, Marc et al. (1995) found that light-adapted goldfish cones contained only slightly more than 100 μM glutamate, suggesting that certain neuronal complexes could indeed still effectively carry out synaptic transmission with a very low steady-state cytosolic glutamate level in the presynaptic element. It has been known for some time, however, that nonmammalian GABAergic horizontal cells release GABA *via* a voltage-sensitive transporter (Schwartz, 1982, 1987; Yazulla and Kleinschmidt, 1983; Ayoub and Lam, 1984), and it is possible that primate horizontal cells do so as well. Our own data show that goldfish horizontal cells are exquisitely sensitive to chronic depolarization and can deplete cytosolic GABA stores completely in minutes (Murry and Marc, 1995). Thus it is plausible that primate horizontal cells are also quite sensitive and may become depleted of GABA under brief anoxia or other circumstances associated with tissue harvest that promote tonic depolarization.

A different problem emerges for amacrine cells. In this and a previous study of amacrine cells (Kalloniatis and Marc, 1992), all central amacrine cells could be classified as γ^+, G^+, or γ^+/G^+. Thus, in goldfish retina (Marc et al., 1995), rat retina (Fletcher and Kalloniatis, 1994), cat retina (Kalloniatis and Tomisich, 1995), chicken retina (Kalloniatis and Fletcher, 1993), and now in central primate retina, all amacrine cells can be nominally assigned to γ^+, G^+, or γ^+/G^+ groups. In the midperiphery and far periphery of the macaque retina, we find some class **X1** (γ^-/G^-) amacrine cells, similar to the results of Koontz et al. (1993), although the fraction of γ^-/G^- cells is smaller (~8% compared with ~30% in Koontz et al., 1993). Differences in tissue harvest conditions might underlie part of this discrepancy. Loss of GABA signals secondary to anesthesia or delay before tissue harvest may artificially produce γ^-/G^- amacrine cell groups in our peripheral samples and in both central and peripheral samples of Koontz et al. (1993). We have observed volatility of horizontal cell GABA signals even when rapid eye removal and fixation were achieved, but we cannot explain why peripheral amacrine cells should be more sensitive than central amacrine cells. We occasionally find **E1** bipolar cells in the amacrine cell layer in peripheral retina, and Koontz et al. (1993) may have classified these as γ^-/G^- amacrine cells, so that the true difference may be even smaller. Finally, small populations of amacrine cells truly lacking any fast amino acid neurotransmitter may yet exist.

The final example of signature heterogeneity is the γ^+ **E3 bipolar cell. The E3** signature is not found in the peripheral retina, even though it is abundant in more central locations, almost exactly paralleling the distributions of γ^+ and γ^- horizontal cells. Grünert and Wässle (1990) also noted a weaker GABA signal in peripheral than in central bipolar cells. GABA-immunoreactive bipolar cells resemble rod bipolar cells in the macaque (Grünert and Martin, 1991), although Vardi and Shi (1996) have argued recently that γ^+ bipolar cells in cat are cone bipolar cells. All evidence supports a single morphological class of rod bipolar cell in mammalian retinas (Polyak, 1941; Boycott and Dowling, 1969; Boycott and Kolb, 1973), with similar labeling patterns for protein kinase C and other macromolecular signals (Grünert and Martin, 1991). All bipolar cells in our samples clearly lack GABA labeling in the periphery. The significance of GABA signals in any bipolar cell remains unknown.

Glutamate precursors: aspartate and glutamine

Aspartate and glutamine distributions in the monkey retina match their likely primary roles as glutamate precursors (Hertz, 1979; Kvamme et al., 1985; Sarthy et al., 1986; Palaiologos et al., 1989; Akiyama et al., 1990; Aoki et al., 1991; Würdig and Kugler, 1991; Gebhard, 1992; Kalloniatis et al., 1994a; Kalloniatis and Napper, 1996). High glutamine levels in Müller's cells arise from recycling of glutamate carbon skeletons via glutamine synthetase (Voaden, 1976, 1978; Riepe and Norenburg, 1977; Hertz, 1979; Moscona, 1983; Pow and Robinson, 1994). Glutamate and aspartate levels generally are well correlated in the monkey retina (Fig. 15), but some glutamatergic neurons such as **E1** photoreceptors and bipolar cells exhibit slightly lower aspartate levels than expected from the trend of **E2**, **E3**, and **E4** cells. Photoreceptors clearly maintain different aspartate/glutamate levels, which as mutual reactants/products of aspartate amino transferase (Altschuler et al., 1982; Mosinger and Altschuler, 1985; Sarthy et al., 1986) should reflect biasing of the transamination toward maintaining higher glutamate and lower aspartate levels through coupled regulation of α-ketoglutarate and oxalacetate levels (for further discussion, see Kalloniatis and Napper, 1996).

Taurine

The high taurine signals in photoreceptors (also see Kuriyama et al., 1990) intimates an important but unknown function. Indeed, taurine deficiency causes photoreceptor degeneration in some mammals (Schmidt et al., 1976; Pasantes-Morales, 1986; Cocker and Lake, 1989). The high content of taurine in Müller's cells is consistent with a multifunctional role, including osmoregulation, stimulation of glycolysis, and gluconeogenesis (Forster et al., 1978; Kulakowski and Maturo, 1984; Ripps and Witkovsky, 1985; Huxtable and Sebring, 1986; Schousboe et al., 1992). Taurine-based osmoregulation may be plausible for photoreceptors, bipolar cells, and Müller's cells, in which uniform taurine contents are found, but it is difficult to understand the existence of multiple groups of γ^+ amacrine cells showing marked differences in taurine content. As for aspartate, however, pattern recognition presents no convincing evidence that taurine has any neurotransmitter role.

Coda

This manuscript primarily addresses neuronal signatures. Because neurons perhaps represent the pinnacle of cellular diversity, they serve as strong tests of the use of pattern recognition in biology; however, even RPE cells and the vascular endothelium possess distinctive signatures, emphasizing that signature analysis may be applied profitably to non-neural tissues and, indeed, in any organism.

REFERENCES

Akiyama H, Kaneko T, Mizuno N, McGeer PL (1990) Distribution of phosphate-activated glutaminase in the human cerebral cortex. J Comp Neurol 297:239–252.

Altschuler RA, Mosinger JL, Harmison GG, Parakkal MH, Wenthold RJ (1982) Aspartate aminotransferase-like immunoreactivity as a marker for aspartate/glutamate in guinea pig photoreceptors. Nature 298:657–659.

Aoki C, Kaneko T, Starr A, Pickel VM (1991) Identification of mitochondrial and non-mitochondrial glutaminase within select neurons and glia of rat forebrain by electron microscopy. J Neurosci Res 28:531–548.

Ayoub GS, Lam DMK (1985) The release of γ-aminobutyric acid from horizontal cells of the goldfish (*Carassius auratus*) retina. J Physiol (Lond) 355:191–214.

Boycott BB, Dowling JE (1969) Organization of the primate retina: light microscopy. Philos Trans R Soc Lond [Biol] 255:109–184.

Boycott BB, Kolb H (1973) The horizontal cells of the rhesus monkey retina. J Comp Neurol 148:115–140.
Cocker SE, Lake N (1989) Effects of dark maintenance on retinal biochemistry and function during taurine depletion in the adult rat. Visual Neurosci 3:33–38.
Cohen E, Sterling P (1986) Accumulation of [^{3}H]glycine by cone bipolar neurons in the cat retina. J Comp Neurol 250:1–7.
Crooks J, Kolb H (1992) Localization of GABA, glycine, glutamate and tyrosine hydroxylase in the human retina. J Comp Neurol 315:287–302.
Dasgupta P, Narayanaswami A (1982) Serine hydroxytransmethylase activity in vertebrate retina. J Neurochem 39:743–746.
Davanger S, Ottersen OP, Storm-Mathisen J (1991) Glutamate, GABA, and glycine in the human retina: an immunocytochemical investigation. J Comp Neurol 311:483–494.
Ehinger B (1989) Glutamate as a retinal neurotransmitter. In: Neurobiology of the inner retina (Weiler R, Osborne NN, eds) pp 1–14. Berlin: Springer.
Ehinger B, Ottersen OP, Storm-Mathisen J, Dowling JE (1988) Bipolar cells in the turtle retina are strongly immunoreactive for glutamate. Proc Natl Acad Sci USA 85:8321–8325.
Fletcher EL, Kalloniatis M (1994) Neuronal and neurochemical architecture of the rat retina. Invest Ophthalmol Vis Sci 35:S1908.
Forster RP, Hannafin JA, Goldstein L (1978) Osmoregulatory role of amino acid in brain of the elasmobranch, *Raja erinacea*. Comp Biochem Physiol [A] 60:25–30.
Gebhard R (1992) Histochemical demonstration of glutamate dehydrogenase and phosphate-activated glutaminase activities in semithin sections of the rat retina. Histochemistry 97:101–103.
Grünert U, Martin PR (1991) Rod bipolar cells in the macaque monkey retina: immunoreactivity and connectivity. J Neurosci 11:2742–2758.
Grünert U, Wässle H (1990) GABA-like immunoreactivity in the macaque monkey retina: a light and electron microscopic study. J Comp Neurol 297:509–524.
Grünert U, Greferath U, Boycott BB, Wässle H (1993) Parasol (Pa) ganglion-cells of the primate fovea: immunocytochemical staining with antibodies against $GABA_A$-receptors. Vision Res 33:1–14.
Hendrickson AE, Koontz MA, Pourcho RG, Sarthy PV, Goebel DJ (1988) Localization of glycine-containing neurons in the Macaca monkey retina. J Comp Neurol 273:473–487.
Hertz L (1979) Functional interactions between neurons and astrocytes I. Turn over and metabolism of putative amino acid transmitters. Prog Neurobiol 13:277–232.
Huxtable RJ, Sebring LA (1986) Towards a unifying theory for the actions of taurine. Trends Pharmacol Sci 7:481–485.
Kalloniatis M, Fletcher E (1993) Immunocytochemical localization of the amino acid neurotransmitters in the chicken retina. J Comp Neurol 336:174–193.
Kalloniatis M, Marc RE (1992) Glutamate, GABA and glycine immunoreactivity in the macaque monkey retina. Soc Neurosci Abstr 18:393.
Kalloniatis M, Napper GA (1996) Glutamate metabolic pathways in displaced ganglion cells of the chicken retina. J Comp Neurol 367:518–536.
Kalloniatis M, Tomisich G (1995) Glycine and GABA in amacrine cells of the cat retina. Invest Ophthalmol Vis Sci 36:S286.
Kalloniatis M, Tomisich G, Marc RE (1994a) Neurochemical signatures revealed by glutamine labeling in the chicken retina. Visual Neurosci 11:793–804.
Kalloniatis M, Marc RE, Tomisich G, Barnes G (1994b) Pathways of glutamate production in the mammalian retina. Invest Ophthalmol Vis Sci 35:S1908.
Kolb H, Nelson R (1983) Rod pathways in the retina of the cat. Vision Res 23:301–312.
Kolb H, Linberg KA, Fisher SK (1992) Neurons of the human retina: a Golgi study. J Comp Neurol 318:147–187.
Koontz MA, Hendrickson LE, Brace ST, Hendrickson AE (1993) Immunocytochemical localization of GABA and glycine in amacrine and displaced amacrine cells of macaque monkey retina. Visual Neurosci 18:2617–2628.
Kulakowski EC, Maturo J (1984) Hypoglycemic properties of taurine: not mediated by enhanced insulin release. Biochem Pharmacol 33:2835–2838.
Kuriyama K, Sasamoto K, Kimura H (1990) A developmental and functional study on taurine-like immunoreactivity in the rat retina. In: Taurine: functional neurochemistry, physiology, and cardiology (Pasantes-Morales H, Martin DL, Shain W, Martín de Río R, eds), pp 29–36. New York: Wiley.
Kvamme E, Torgner IAA, Svenneby G (1985) Glutaminase from mammalian tissues. Methods Enzymol 113:241–256.
Marc RE (1989) The role of glycine in the mammalian retina. In: Progress in retinal research, Vol 8 (Osborne N, Chader G, eds), pp 67–107. London: Pergamon.
Marc RE (1996) Mapping glutamate drive in retinal neurons with AGB: a probe of cation channel activation. Invest Ophthalmol Vis Sci 37:S654.
Marc RE, Liu W-LS (1985) Glycine-accumulating neurons in the human retina. J Comp Neurol 232:241–260.
Marc RE, Liu W-LS, Kalloniatis M, Raiguel S, Van Haesendonck E (1990) Patterns of glutamate immunoreactivity in the goldfish retina. J Neurosci 10:4006–4034.
Marc RE, Murry RF, Basinger SF (1995) Pattern recognition of amino acid signatures in retinal neurons. J Neurosci 15:5106–5129.
Martin PR, Grünert U (1992) Spatial density and immunoreactivity of bipolar cells in the macaque monkey retina. J Comp Neurol 323:269–287.
Massey SC (1990) Cell types using glutamate as a neurotransmitter in the vertebrate retina. In: Progress in retinal research, Vol 9 (Osborne NN, Chader G,eds), pp 399–425. London: Pergamon.
Miller SS, Steinberg RH (1976) Transport of taurine, L-methionine and 3-O-methyl-D-glucose across the frog retinal pigment epithelium. Exp Eye Res 23:177–189.
Montero VM, Wenthold RJ (1989) Quantitative immunogold analysis reveals high glutamate levels in retinal and cortical synaptic terminals in the lateral geniculate nucleus of the macaque. Neuroscience 31:639–647.
Moscona AA (1983) On glutamine synthetase, carbonic anhydrase and Müller glia in the retina. In: Progress in retinal research, Vol 2 (Osborne N, Chader G, eds), pp 111–135. Oxford: Pergamon.
Mosinger JL, Altschuler RA (1985) Aspartate aminotransferase-like immunoreactivity in the Guinea Pig and Monkey retina. J Comp Neurol 233:255–268.
Muller JF, Marc RE (1990) GABA-ergic and glycinergic pathways in the inner plexiform layer of the goldfish retina. J Comp Neurol 291:281–304.
Murry RF, Marc RE (1995) Glutamatergic driving of amacrine and bipolar cell populations in the goldfish retina. Invest Ophthalmol Vis Sci 36:S383.
Ottersen OP, Zhang N, Walberg F (1992) Metabolic compartmentation of glutamate and glutamine: morphological evidence obtained by quantitative immunocytochemistry in rat cerebellum. Neuroscience 46:519–534.
Palaiologos G, Hertz L, Schousboe A (1989) Role of aspartate aminotransferase and mitochondrial dicarboxylate transport for release of endogenously supplied neurotransmitter in glutamatergic neurons. Neurochem Res 14:359–366.
Pasantes-Morales H (1986) Current concepts on the role of taurine in the retina. In: Progress in retinal research, Vol 5 (Osborne NN, Chader GJ, eds), pp 207–229. Oxford: Pergamon.
Pautler EL, Tengerdy C (1986) Transport of acidic amino acids by the bovine pigment epithelium. Exp Eye Res 43:207–214.
Polyak SL (1941) The retina. Chicago: University of Chicago.
Pourcho R, Goebel DJ (1987) Visualization of endogenous glycine in the cat retina: an immunocytochemical study with Fab fragments. J Neurosci 7:1189–1197.
Pow DV, Robinson SR (1994) Glutamate in some retinal neurons is derived solely from glia. Neuroscience 60:355–366.
Richards JA (1993) Remote sensing digital image analysis. Berlin: Springer.
Riepe RE, Norenburg MD (1977) Müller cell localisation of glutamine synthetase in rat retina. Nature 268:654–655.
Ripps H, Witkovsky P (1985) Neuron-glia interaction in the brain and retina. In: Progress in retinal research, Vol 4 (Osborne NN, Chader GJ, eds), pp 181–219. Oxford: Pergamon.
Robin LM, Kalloniatis M (1992) Interrelationship between retinal ischemic damage and turnover and metabolism of putative amino acid neurotransmitters, glutamate and GABA. Doc Ophthalmol 30:273–300.
Salceda R, Saldaña MR (1993) Glutamate and taurine uptake by retinal pigment epithelium during rat development. Comp Biochem Physiol 104C:311–316.
Sarthy PV, Hendrickson AE, Wu JY (1986) L-glutamate: a neurotransmitter candidate for cone photoreceptors in the monkey retina. J Neurosci 6:637–643.

Schmidt SY, Berson EL, Hayes KC (1976) Retinal degeneration in cats fed casein. I. Taurine deficiency. Invest Ophthalmol Vis Sci 15:47–52.

Schousboe A, Apreza CL, Pasantes-Morales H (1992) GABA and taurine serve as respectively a neurotransmitter and an osmolyte in cultured cerebral cortical neurons. In: Taurine (Lombardini JB, Schaffer SW, Azuma J, eds), pp 391–397. New York: Plenum.

Schwartz EA (1982) Calcium-independent release of GABA from isolated horizontal cells of the toad retina. J Physiol (Lond) 323:211–227.

Schwartz EA (1987) Depolarization without calcium can release γ-aminobutyric acid from a retinal neuron. Science 238:350–354.

Shank RP, Campbell GL (1984a) α-Ketoglutarate and malate uptake and metabolism by synaptosomes: further evidence for an astrocyte to neuron metabolic shuttle. J Neurochem 42:1153–1161.

Shank RP, Campbell GL (1984b) Glutamine glutamate and other possible regulators of α-ketoglutarate and malate uptake. J Neurochem 42:1162–1169.

Swain PH, Davis SM (1978) Remote sensing: a quantitative approach. New York: McGraw-Hill.

Vaney DI (1990) The mosaic of amacrine cells in the mammalian retina. In: Progress in retinal research, Vol 9 (Osborne N, G Chader, eds), pp 49–100. London: Pergamon.

Vardi N, Shi J-Y (1996) Identification of GABA containing bipolar cells in cat retina. Invest Ophthalmol Vis Sci 37:S418.

Vardi N, Sterling P (1994) Subcellular localization of $GABA_A$ receptors on bipolar cells in Macaque and human retina. Vision Res 34:1235–1246.

Vardi N, Kaufman DL, Sterling P (1994) Horizontal cells in cat and monkey retina express different isoforms of glutamic acid decarboxylase. Vis Neurosci 11:135–142.

Voaden MJ (1976) Gamma-aminobutyric acid and glycine as retinal neurotransmitters. In: Transmitters in the visual process (Bonting SL, ed), pp 107–125. Oxford: Pergamon.

Voaden MJ (1978) Localization and metabolism of neuroactive amino acids in the retina. In: Amino acids as chemical transmitters (Fonnum F, ed), pp 257–274. New York: Plenum.

Wässle H, Boycott BB (1991) Functional architecture of the mammalian retina. Physiol Rev 71:447–480.

Wässle H, Grünert U, Röhrenbeck J, Boycott BB (1990) Retinal ganglion cell density and cortical magnification factor in the primate. Vision Res 30:1897–1911.

Wässle H, Grünert U, Chun M-H, Boycott BB (1995) The rod pathway of the macaque monkey retina: identification of AII-amacrine cells with antibodies against calretinin. J Comp Neurol 361:537–551.

Wilson JR, Cowey A, Somogyi P (1996) GABA immunopositive axons in the optic nerve and optic tract of Macaque monkeys. Vision Res 36:1357–1363.

Würdig S, Kugler P (1991) Histochemistry of glutamate metabolizing enzymes in the rat cerebellar cortex. Neurosci Lett 130:165–168.

Yazulla S (1986) GABAergic mechanisms in retina. In: Progress in retinal research, Vol 5 (Osborne NN, Chader GJ, eds), pp 1–52. New York: Pergamon.

Yazulla S, Kleinschmidt J (1983) Carrier mediated release of GABA from retinal horizontal cells. Brain Res 263:63–75.

Yu BC-Y, Watt CB, Lam DMK, Fry KR (1988) GABAergic ganglion cells in the rabbit retina. Brain Res 439:376–382.

Zhang L, Kalloniatis M, Marc RE, Kolb H (1996) Calretinin immunostaining in the monkey fovea. Invest Ophthalmol Vis Sci 37:S950.